



Pigments—copper-based greens and blues

Silvie Švarcová¹ · David Hradil^{1,2} · Janka Hradilová² · Zdeňka Čermáková¹

Received: 30 January 2021 / Accepted: 30 June 2021 / Published online: 13 October 2021
© The Author(s), under exclusive licence to Springer-Verlag GmbH Germany, part of Springer Nature 2021

Abstract

Since antiquity, various copper-containing substances have been used as green and blue pigments. Their exceptional diversity, reflecting their various chemical and phase composition, chemical stability as well as their origin, makes their correct identification challenging. The review focuses on copper-based pigments used in ancient and mediaeval works of art, especially in wall paintings and/or related polychromed decorations or statues—siliceous copper pigments (Egyptian blue and green, Han blue and purple, chrysocolla), copper carbonates (azurite, malachite, blue and green verditers), copper chlorides (atacamite-group, cumengeite, calumetite), copper sulphates (posnjakite, brochantite) and—to a lesser extent—copper acetates (verdigris) and other organometallics. Particular attention is given to the necessity of the detailed study of accompanying phases which can serve as useful indicators of natural and/or artificial origin of copper pigments. Factors affecting the stability of copper pigments in wall paintings—salt attack, oxalic acid, alkalinity and heat—are overviewed. A suitable analytical approach based on complementary combination of in situ and laboratory analyses for proper identification and differentiation of copper pigments is proposed.

Keywords Copper pigments · Wall paintings · Origin · Degradation · Analysis

Premise

This Topical Collection (TC) covers several topics in the field of study, in which ancient architecture, art history, archaeology and material analyses intersect. The chosen perspective is that of a multidisciplinary scenario, capable of combining, integrating and solving the research issues raised by the study of mortars, plasters and pigments (Gliozzo et al. 2021).

The first group of contributions explains how mortars have been made and used through the ages (Arizzi and Cultrone 2021; Ergenç et al. 2021; Lancaster 2021; Vittì 2021). An insight into their production, transport and on-site organisation is further provided by DeLaine (2021). Furthermore, several issues concerning the degradation and conservation of mortars and plasters are addressed from practical and technical standpoints (La Russa and Ruffolo 2021; Caroselli et al. 2021).

The second group of contributions is focused on pigments, starting from a philological essay on terminology (Becker 2021). Three archaeological reviews on prehistoric (Domingo Sanz and Chieli 2021), Roman (Salvadori and Sbrolli 2021) and mediaeval (Murat 2021) wall paintings clarify the archaeological and historical/cultural framework. A series of archaeometric reviews illustrate the state of the art of the studies carried out on Fe-based red, yellow and brown ochres (Mastrotheodoros et al. 2021), Cu-based greens and blues (this paper), As-based yellows and reds (Gliozzo and Burgio 2021), Pb-based whites, reds, yellows and oranges (Gliozzo and Ionescu 2021), Hg-based red and white (Gliozzo 2021) and organic pigments (Aceto 2021). An overview of the use of inks, pigments and dyes in manuscripts, their scientific examination and

This article is part of the Topical Collection on *Mortars Plasters and pigments: Research questions and answers*

✉ Silvie Švarcová
svarcova@iic.cas.cz

David Hradil
hradil@iic.cas.cz

Janka Hradilová
hradilovaj@volny.cz

Zdeňka Čermáková
cermakova@iic.cas.cz

¹ ALMA Laboratory, Institute of Inorganic Chemistry, Czech Academy of Sciences, Husinec 1001, 25068, Husinec-Řež, Czech Republic

² ALMA Laboratory, Academy of Fine Arts in Prague, U Akademie 4, 170 22 Praha 7, Czech Republic

analysis protocol (Burgio 2021) as well as an overview of glass-based pigments (Cavallo and Riccardi 2021) are also presented. Furthermore, two papers on cosmetic (Pérez-Arantegui, 2021) and bioactive (antibacterial) pigments (Knapp et al. 2021) provide insights into the variety and different uses of these materials.

Introduction

Since ancient times, various copper compounds have been used as blue and green pigments and dyes. Copper pigments include natural minerals, such as malachite and azurite, their artificial analogues (the so-called verditers), various basic copper chlorides and/or sulphates of ambiguous origin, as well as synthetic pigments—e.g. ancient Egyptian blue, mediaeval verdigris (copper acetates), modern emerald and Scheele greens, or, most recently, phthalocyanine. The diverse composition of copper-based pigments is illustrated by Table 1, while the variety of green and blue hues of natural and artificial mediaeval copper pigments is shown in Fig. 1. It is astonishing, how the list of historic copper pigments has been still extended and new pieces of knowledge have been emerged, profiting from increasing quality and availability of instrumental analytical techniques and interdisciplinary scientific research of cultural heritage. Thus, besides best known pigments such as azurite, malachite (Gettens and FitzHugh 1993a, b), verdigris (Kühn 1993) or Egyptian blue (Riederer 1997), we can find more and more evidences about the use of less frequent copper chlorides and sulphates. Presuming that historic copper pigments of both natural and artificial origin are not usually phase-pure substances but they commonly consist of colour-bearing and numerous other accompanying phases, detailed and targeted analyses can reveal indicators of the pigments' provenance, manufacturing procedure or degradation. The aim of this paper is to overview copper pigments used in ancient and mediaeval times, especially in wall paintings and related polychromed objects, and to emphasise the importance of recognition of subtle details hidden in paint layers.

The basic facts about copper pigments used in ancient and mediaeval wall paintings and/or related polychromed objects are overviewed in the “[Copper pigments used in ancient and mediaeval wall paintings](#)” section. The various aspects of their genesis, involving the indicators of natural origin and reconstruction of manufacturing of artificial pigments are discussed on the basis of reported scientific research in the “[Origin of copper-based pigments](#)” section. Finally, the substantial phenomena affecting the stability of copper pigments are compiled in the “[Degradation of copper-based pigments](#)” section.

Copper pigments used in ancient and mediaeval wall paintings

Siliceous copper pigments

Pigments containing copper (Cu) and silicon (Si) in their structure are counted among silicates (e.g. synthetic Egyptian blue, Han blue and purple, or natural chrysocolla) or silica glasses (e.g. Egyptian green) (Scott 2016; Riederer 1997). However, ancient artificial pigments often vary in chemical and/or phase composition depending on the actual manufacturing conditions. Therefore, they can differ in crystallinity as well as presence of various by-products or unreacted compounds. For example Egyptian blue, widely considered to be calcium copper silicate, is rather a mixture of several crystalline and glassy phases. The siliceous copper substances are assumed to be the most stable copper pigments, nevertheless, changes in their appearance and/or chemical composition have been reported, e.g. in connection with salt attack or the alteration of binders (Coccatto et al. 2017).

Egyptian blue

Egyptian blue, the first ingenious man-made pigment ever and the most successful blue artificial pigment in history, had been widely employed for 3000 years. It had been used from about the Fourth Dynasty (ca. 2639–2504 BCE) till the Roman period (332 BCE–395 CE), adorning wood, papyrus, stone, cartonnage, stucco, plaster, and metallic objects (Riederer 1997; Scott 2016). The area of use of Egyptian blue covers the Mediterranean basin (Egypt, West Asia, Greece, Italy and Roman sites), while it has not been found in the pigments analysed from the historical sites of India, Central and East Asia (Riederer 1997).

Customarily, the term Egyptian blue refers to $\text{CaCuSi}_4\text{O}_{10}$ corresponding to the mineral cuprorivaite; however, the numerous analyses of the preserved pigment specimens excavated in various archaeological sites indicate varied mixtures (David et al. 2001; Pagès-Camagna and Colinart 2003; Shortland 2006; Pradell et al. 2006; Hatton et al. 2008). In addition to the colour-bearing cuprorivaite phase (Pagès-Camagna et al. 2006), Egyptian blue can consist of silicon oxides in the form of quartz, tridymite or cristobalite, copper alkali-bearing silica glass phases, wollastonite (CaSiO_3), occasionally copper oxides (cuprite, Cu_2O , or tenorite, CuO) or unreacted bronze fragments, and minor phases containing sodium, potassium, aluminium, iron, tin, arsenic or lead (Riederer 1997; Scott 2016). The presence and abundance of particular phases reflect the technological process, especially the choice/

Table 1 Copper-based pigments

Group	Name of pigment	Colour-bearing phase	Possible additional phases	Approx. period of use in paintings
Siliceous	Egyptian blue	$\text{CaCuSi}_4\text{O}_{10}$ (cuprorivaite)	Quartz, cristobalite, tridymite (SiO_2); (para)wollastonite (CaSiO_3); alkali silica copper glass; tenorite (CuO); cuprite (Cu_2O); metal residues (copper, bronze); minor components with Na, K, Al, Fe, Sn, As, Pb	2600 BCE–400 CE occasionally 5th–12th c. CE
	Chinese blue	$\text{BaCuSi}_4\text{O}_{10}$	PbCO_3 , other Ba-Cu-Si-(Sn) phases	500 BCE–220 CE
	Chinese purple	$\text{BaCuSi}_2\text{O}_6$ (blue) + Cu_2O (cuprite, red)	PbCO_3 , other Ba-Cu-Si-(Sn) phases	500 BCE–220 CE
	Chrysocolla	$(\text{Cu}, \text{Al})_2\text{H}_2\text{Si}_2\text{O}_5(\text{OH})_4 \cdot n\text{H}_2\text{O}$		Undeterminable
	Egyptian green	Silica-rich copper glass	(Para)wollastonite (CaSiO_3); cristobalite, quartz (SiO_2); metal residues	2100 BCE–400 CE
Carbonates	Azurite	$\text{Cu}_3(\text{CO}_3)_2(\text{OH})_2$	Malachite; cuprite (Cu_2O); pseudomalachite ($\text{Cu}_5(\text{PO}_4)_2(\text{OH})_4$); Cu/Zn arsenates; Fe-oxides; Ti-oxides; barite (BaSO_4); Sb-oxides; aluminosilicates	2600 BCE–1800 CE
	Blue verditer	$\text{Cu}_3(\text{CO}_3)_2(\text{OH})_2$ (azurite structure)		17th–19th c. CE
	Malachite	$\text{Cu}_2(\text{CO}_3)(\text{OH})_2$	Azurite + the same minerals as for azurite	2600 BCE–1900 CE
	Green verditer	$\text{Cu}_2(\text{CO}_3)(\text{OH})_2$ (malachite structure)		Since middle ages
Chlorides	Atacamite*	$\text{Cu}_2\text{Cl}(\text{OH})_3$	Malachite (spherulitic), Cu-S-(Cl) phases	Undeterminable
	Botallackite*	$\text{Cu}_2\text{Cl}(\text{OH})_3$		Undeterminable
	Clinoatacamite*	$\text{Cu}_2\text{Cl}(\text{OH})_3$		Undeterminable
	Paratacamite*	$\text{Cu}_2\text{Cl}(\text{OH})_3$	Malachite (spherulitic), Cu-S-(Cl) phases	Undeterminable
	Calumetite	$\text{Cu}(\text{OH}, \text{Cl}) \cdot 2\text{H}_2\text{O}$		Undeterminable
	Cumengeite	$\text{Pb}_{21}\text{Cu}_{20}\text{Cl}_{42}(\text{OH})_{40}$		Undeterminable
Sulphates	Antlerite	$\text{Cu}_3(\text{SO}_4)(\text{OH})_4$		Undeterminable
	Brochantite	$\text{Cu}_4(\text{SO}_4)(\text{OH})_6$	Malachite (spherulitic), Cu-Cl-(S) phases	Undeterminable
	Langite	$\text{Cu}_4(\text{SO}_4)(\text{OH})_6 \cdot 2\text{H}_2\text{O}$		Undeterminable
	Posnjakite	$\text{Cu}_4(\text{SO}_4)(\text{OH})_6 \cdot \text{H}_2\text{O}$	Malachite (spherulitic), Cu-Cl-(S) phases	Undeterminable
As-containing compounds	Emerald green	$\text{Cu}_4(\text{CH}_3\text{COO})_2(\text{AsO}_2)_2$		Since the 19th c. CE
	Scheele's green	$2\text{-}3\text{CuO} \cdot \text{As}_2\text{O}_3 \cdot 2\text{H}_2\text{O}$		18th–19th c. CE
Acetates	Verdigris neutral	$\text{Cu}(\text{CH}_3\text{COO})_2 \cdot \text{H}_2\text{O}$ (hoganite)		?–19th c. CE
	Basic verdigris	See Table 3		?–19th c. CE
Organometallics	Copper resinat	Cu salts of resin acids		17th–19th c. CE
	Oleates, proteينات			Undeterminable
	Wax complexes			Undeterminable
	Phthalocyanine blue	$\text{C}_{32}\text{H}_{16}\text{N}_8\text{Cu}$		Since the 20th c. CE
	Phthalocyanine green	$\text{C}_{32}\text{H}_2\text{N}_8\text{Cl}_{14}\text{Cu}$		Since the 20th c. CE

*Polymorphs differing by crystal structure

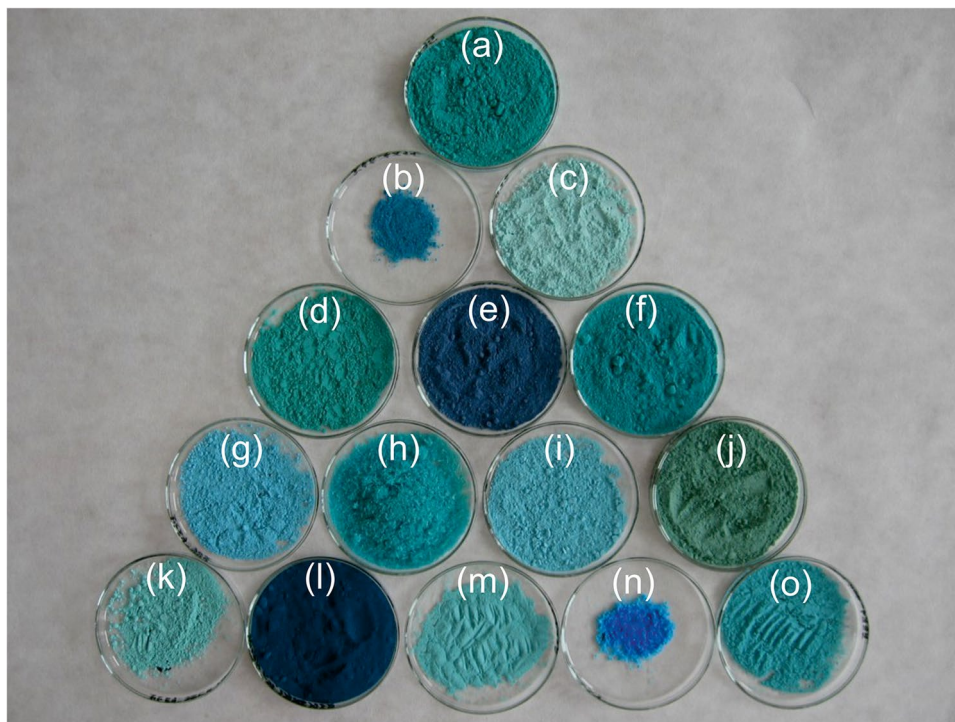


Fig. 1 Variety of mediaeval natural and artificial copper-based pigments: **a** artificial “best blue”, a complex mixture of unidentified products resulting from mixing of NH_4Cl and $\text{Cu}(\text{CH}_3\text{COO})_2 \cdot \text{H}_2\text{O}$ in volume ratio 3:6, resp., prepared by authors following instructions from the fifteenth century manuscript *MS 1243*, Bibliotheca Riccardiana, Padua, Italy (Scott 2002, pp 285); **b** undefined mixture of copper acetates collected from copper plates exposed to vinegar fumes, authors’ unpublished results; **c** artificial “mountain blue”, a mixture of gypsum [$\text{CaSO}_4 \cdot 2\text{H}_2\text{O}$], atacamite [$\text{Cu}_2\text{Cl}(\text{OH})_3$] and posnjakite [$\text{Cu}_4\text{SO}_4(\text{OH})_3 \cdot \text{H}_2\text{O}$] resulting from mixing of CuSO_4 , CaCl_2 and $\text{Ca}(\text{OH})_2$, prepared by authors following the description for preparation of artificial azurite by Šimůnková and Bayerová (2014, pp 79), unpublished results; **d** artificial malachite [$\text{Cu}_2(\text{CO}_3)(\text{OH})_2$] prepared by precipitation (Švarcová et al. 2009); **e** natural azurite [$\text{Cu}_3(\text{CO}_3)_2(\text{OH})_2$], Kremer Pigmente; **f** artificial “best blue”, a complex mixture of unidentified products resulting from mixing of NH_4Cl and $\text{Cu}(\text{CH}_3\text{COO})_2 \cdot \text{H}_2\text{O}$ in volume ratio 1:3, resp., prepared by authors following instructions from the fifteenth century manu-

script *MS 1243*, Bibliotheca Riccardiana, Padua, Italy (Scott 2002, pp 285), unpublished results; **g** artificial “mountain blue”, a mixture of gypsum [$\text{CaSO}_4 \cdot 2\text{H}_2\text{O}$], atacamite [$\text{Cu}_2\text{Cl}(\text{OH})_3$], devilline [$\text{CaSO}_4 \cdot \text{Cu}_4\text{SO}_4(\text{OH})_6 \cdot \text{H}_2\text{O}$], $\text{CaCO}_3 \cdot \text{H}_2\text{O}$ and malachite [$\text{Cu}_2(\text{CO}_3)(\text{OH})_2$], resulting from mixing of CuSO_4 , CaCl_2 , $\text{Ca}(\text{OH})_2$ and K_2CO_3 prepared by authors adapting the description for preparation of artificial azurite by Šimůnková and Bayerová (2014, pp 79), unpublished results; **h** mixture of artificial brochantite [$\text{Cu}_4(\text{SO}_4)(\text{OH})_6$] and malachite [$\text{Cu}_2(\text{CO}_3)(\text{OH})_2$] prepared by precipitation (Švarcová et al. 2012); **i** $\text{CuCl}_2 \cdot 2\text{H}_2\text{O}$, LachNer Chemicals; **j** malachite natural [$\text{Cu}_2(\text{CO}_3)(\text{OH})_2$], Kremer Pigmente; **k** artificial posnjakite [$\text{Cu}_4(\text{SO}_4)(\text{OH})_6 \cdot \text{H}_2\text{O}$] prepared by precipitation (Švarcová et al., 2009); **l** neutral copper acetate [$\text{Cu}(\text{CH}_3\text{COO})_2 \cdot \text{H}_2\text{O}$], LachNer Chemicals; **m** artificial paratacamite [$\text{Cu}_2\text{Cl}(\text{OH})_3$] prepared by precipitation (Švarcová et al. 2012); **n** undefined mixture of copper acetates collected from copper plates exposed to vinegar fumes (authors’ unpublished results); **o** artificial malachite [$\text{Cu}_2(\text{CO}_3)(\text{OH})_2$] prepared by precipitation (Švarcová et al. 2009), different batch than in **d**

availability of the raw materials, their proportion and temperature achieved during the synthesis. Generally, the pigment can be prepared by heating the raw materials (Cu-containing ores or metal scraps, lime and silica sand) together with a few percent of flux (soda, potash, etc.) to temperatures between 800 and 1100 °C (Pagès-Camagna and Colinart 2003; Berke 2007).

The use of Egyptian blue lasted sporadically till the Middle Ages as evidenced by its identification in several wall paintings from the fifth to the ninth century, as overviewed by Riederer (1997). Later on, its manufacturing technology had been completely abandoned or forgotten (Orna et al. 1980). However, the exceptional association of Egyptian blue with ultramarine blue in early mediaeval

wall paintings was recently reported by Cavallo et al. (2020). Even later re-use of Egyptian blue was reported by Pozza et al. (2000), Lluveras et al. (2010a) or Bredal-Jørgensen et al. (2011). In such cases, finding of Egyptian blue on mediaeval paintings can be interpreted as an accidental use of pigments’ remnants from the former Roman settlements (Lluveras et al. 2010a).

Egyptian green

Egyptian green, sometimes also called the “green frit”, can exhibit a range of colours from green through turquoise to pale blue, reflected by the various terms referring to the pigment (Hatton et al. 2008). In comparison to its blue

counterpart, Egyptian green was much less known for a long time (Scott 2016), although its existence and intentional production has been proposed by scientists since the 1970s (Riederer 1997). It had been believed that, contrary to Egyptian blue, the green pigment had not been used outside the Egyptian territory (Scott 2016) as it was found on artefacts from 2100 to 1069 BCE corresponding to the Middle and New Kingdoms (Pagès-Camagna and Colinart 2003; Moussa et al. 2009). However, Perez-Rodriguez et al. (2015) reported presence of Egyptian green in the fragments of Roman mural paintings in the Royal Alcazars of Seville, Spain. Similarly to Egyptian blue, the green pigment is a heterogeneous material; however, the colour-bearing phase is silica-rich copper glass (Pagès-Camagna et al. 2006), predominantly accompanied by parawollastonite (CaSiO_3 polymorph formed between 950 and 1150 °C) and possibly other minor phases (e.g. cristobalite, quartz, metal residues etc.). The final composition depends on both the raw materials and the firing temperature as evidenced in an extensive study of both the archaeological pigment specimens and the technological replicas performed by Pagès-Camagna and Colinart (2003). The authors demonstrated that the synthetic procedure is close to that of Egyptian blue, but it differs in higher Ca/Cu ratio as well as higher amount of flux in the starting mixture.

Chinese (Han) blues and purple

Chinese blue and purple barium copper silicate pigments were invented in northern China probably not earlier than 800 BCE (Berke 2007). The pigments were first evidenced on ancient artefacts by FitzHugh and Zycherman (1983, 1992) who termed them “Han”. They were identified on artefacts from the Warring States Period (475–221 BCE) and the Han Dynasty (208 BCE–220 CE) (Berke 2007; Xia et al. 2014; Zhang et al. 2019). The similarity of the composition and manufacturing of the Chinese pigments to Egyptian blue is astonishing, although they were probably invented independently. The colour-bearing phase of Han blue, $\text{BaCuSi}_4\text{O}_{10}$, is a structural analogue of cuprorivaite, differing only by the presence of Ba ions instead of Ca. In their crystal structure, copper ions (playing the role of chromophores) are very tightly bound in the stable silicate matrix and cannot be removed easily by chemical and physical means, resulting in the high stability of Egyptian and Han blue (Berke 2007). On the contrary, the crystal structure of colour-bearing phase of Han purple, $\text{BaCuSi}_2\text{O}_6$, differs significantly. It contains an untypical copper–copper bond responsible for the low chemical stability of the pigment (Berke 2007). Similarly to Egyptian pigments, their Chinese counterparts were produced by heating the raw materials involving barium minerals (barite, BaSO_4 , or witherite, BaCO_3), silica sand (SiO_2), copper minerals (e.g. malachite,

$\text{Cu}_2(\text{CO}_3)(\text{OH})_2$) and lead flux additives (Pb oxides or carbonates) to temperatures 900–1000 °C. Thus, the final products also consist of additional components formed during the heat treatment of the starting mixture, especially lead-based phases (oxides and carbonates) are reported as the residues of flux (Berke 2007; Xia et al. 2014). It is noteworthy that the purple hue of Han purple is caused by the presence of red copper(I) oxide (Cu_2O , cuprite) which is slowly generated by the decomposition of $\text{BaCuSi}_2\text{O}_6$ (Berke 2007). Recently, Chinese dark blue ($\text{BaCu}_2\text{Si}_2\text{O}_7$) and pabstite ($\text{BaSnsi}_3\text{O}_9$) have been identified as additional phases together with Han blue and/or purple by Xia et al. (2014) and Zhang et al. (2019), illustrating the diversity of the products.

Chrysocolla

The extent of the use of the naturally occurring poorly crystalline blue-green copper mineral chrysocolla, $(\text{Cu,Al})_2\text{H}_2(\text{Si}_2\text{O}_5)(\text{OH})_4 \cdot n(\text{H}_2\text{O})$, as a pigment is questionable (Scott 2016). In the antiquity, it was used as an ingredient to solder gold, which is reflected in its name derived from the Greek words for gold (chrysos) and glue (kolla). However, the term chrysocolla can also refer to malachite in the classical and mediaeval literature (Gettens and FitzHugh 1993a). Scott (2016) pointed out that the determination of its presence can be troublesome because of varying optical characteristics and the degree of crystallinity which can result in confusion, for example with Egyptian green. The use of chrysocolla as a pale blue pigment was reported by Mugnaini et al. (2006), who identified it in the draperies on the thirteenth century wall paintings excavated under the floor of the cathedral in Siena, Italy.

Basic copper carbonates

Basic copper carbonates, blue azurite ($\text{Cu}_3(\text{CO}_3)_2(\text{OH})_2$) and green malachite ($\text{Cu}_2(\text{CO}_3)(\text{OH})_2$), are the best known and wide-spread representatives of copper mineral-type pigments, and had been used since antiquity till the modern era (Gettens and FitzHugh 1993a,b). Both mineral pigments have their artificial analogues called “verditer” or “bice”, having identical chemical composition as well as crystal-line structure, but differing by circular habitus of their crystal particles. However, while the artificial malachite can be found already in mediaeval artworks (Švarcová et al. 2009), the artificial azurite appeared later on—in the seventeenth century (MacTaggart and MacTaggart 1980).

Azurite and malachite

Azurite was the most important blue pigment in mediaeval European painting up to the seventeenth century; its wide-spread use was closely linked to the development of Cu-ore

mining in Europe, and it was significantly favoured due to its lower price compared to natural ultramarine, a pigment separated from lapis lazuli, which was imported from the present-day Afghanistan and which was preferably used in Mediterranean. Efforts to gradually replace it date back to the sixteenth century: at first, it was substituted by the newly available smalt (Co-containing glass), which, however, did not exactly have the same colour and intensity. Instead, azurite was being “faded” with smalt in various proportions, as evidenced by a number of examples (Fig. 2). In the Flemish countries, for example azurite was mixed also with indigo (organic blue dyestuff extracted from the leaves of some plants of the *Indigofera* genus). An almost complete replacement of mineral azurite in Europe at the beginning of the eighteenth century was caused by the expansion of Prussian blue in the painting. Besides Europe, azurite was also the most important blue pigment of the Far East (Gettens and FitzHugh 1993b). Very early evidence of the use of azurite was reported by Çamurcuoğlu (2015), who found it in a burial context at Neolithic Central Anatolian Site—however, not as the material for wall paintings, but probably as cosmetic. Although azurite pigment was known in ancient Egypt (David et al. 2001), it was not widely used there because of the easy availability of artificial Egyptian blue (Gettens and FitzHugh 1993b; Scott 2016).

Despite its higher abundance in nature, malachite is less commonly mentioned in the art literature than azurite (Gettens and FitzHugh 1993a), which is probably caused by the simultaneous availability of other green pigments such as artificial verdigris or natural green earths (celadonite, glauconite). In ancient and mediaeval artworks, it would be beneficial to distinguish in which regions the green

earth was prevailing and in which the Cu pigments were preferentially used. According to yet unpublished and fragmentary evidences it corresponds with the availability of these minerals—while the green earth was more frequent in Southern Europe, because of rich sources of celadonite near Verona, Italy, and in Cyprus, in Central Europe Cu pigments prevailed. Generally, malachite is accompanying azurite in nature, which constitutes a precondition of their use in the same historical periods. It almost disappeared in the nineteenth century because of the availability of cheaper synthetic greens (emerald green, Scheele green, chromium green etc.). In addition, malachite was used abundantly also in the Far East (Gettens and FitzHugh 1993a) and in ancient Egypt, where it represented the most common cosmetics; however, it was also used in paintings as evidenced by its identification in numerous artefacts (Scott 2016).

Regarding their natural origin, both minerals form as secondary minerals in the upper weathered (oxidation) zones of copper ore deposits, usually in mutual associations, accompanied by other copper-rich and other minerals (Table 1) (Hradil et al. 2008; Aru et al. 2014). With respect to their geological formation, both minerals were most typically exploited as secondary products of copper mining. Preparation of minerals for pigment use typically involved grounding of mineral lumps followed by washing, levigating and sieving of the powders. While the coarsely ground mineral produces dark hues, the fine grinding results in lighter tones (Gettens and FitzHugh 1993a). Significant mediaeval sources of azurite and malachite are documented in today’s Slovakia (namely, Lubietová and Špania Dolina in Banská Bystrica mining district), which was mentioned in the written sources dating from the thirteenth to the nineteenth century, and also French deposits in Chessy near Lyon (Gettens and FitzHugh 1993a,b; Heydenreich et al. 2005; Velebil 2008; Heydenreich 2013).

Blue and green verditer (artificial azurite and malachite)

Both azurite and malachite have their artificial analogues. Blue verditer or blue bice are terms for artificial azurite and, similarly, green verditer or green bice denote the artificial malachite. However, many of the terms applied to azurite and malachite (that is mountain blue, mountain green and their linguistic variants) have also been used to describe the blue and the green verditer and vice versa. Van Loon and Speelers (2011), who identified both verditers in the mid-seventeenth century oil paintings in Oranjezaal, The Hague (the Netherlands), pointed out that the indefinable colour of the verditer products, varying between blue and green, was reflected in the vague terminology of the contemporary (i.e. the seventeenth century) treatises. Nomenclature confusion of copper carbonates and copper silicates was also common. As mentioned above, malachite is often referred to

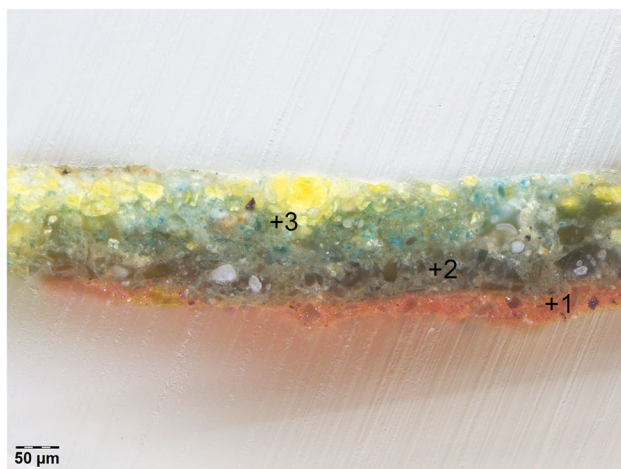


Fig. 2 Azurite and smalt used together in original layers of oil-on-canvas painting *St. John the Baptist with his Follower* dated to the seventeenth century, Třeboň Castle, Czech Republic; simplified description of layer stratigraphy on the micro-section in visible light: 1 clay-based ground, 2 smalt, 3 azurite mixed with massicot

as chrysocolla in classical and mediaeval treatises (Gettens and FitzHugh 1993a; Heydenreich et al. 2005).

Green verditer (artificial malachite) can be prepared by precipitation: adding sodium bicarbonate/carbonate into copper sulphate/nitrate solution or combining copper nitrate with chalk, resulting in a pale green product of distinctively spherulitic crystal habit, which are almost uniform in size (Naumova et al. 1990; Gettens and FitzHugh 1993a; Švarcová et al. 2009). However, spherulitic particles do not automatically prove the synthetic origin of the pigment. Heydenreich et al. (2005) reported the formation of spherulitic mineral malachite by natural precipitation from copper mine flowing water or on tailings, describing the situation in the above-mentioned Banská Bystrica region (Slovakia).

Preparation of the blue verditer has been described similarly to green verditer (Gettens and FitzHugh 1993b). However, in contrast to artificial malachite, the actual artificial azurite with typical spherulitic particles was probably produced and used later, being a by-product of silver and gold refiners' craft in England (MacTaggart and MacTaggart 1980). MacTaggart experimentally demonstrated that the character of the end product depends on reaction conditions, especially on the temperature and the stirring; while blue verditer required precipitation at low temperatures (not above 12–16 °C), the green one forms easily under wide range of conditions. Besides the seventeenth century paintings in Oranjezaal (Van Loon and Spellers 2011), the blue verditer is reported as a well-established pigment used by interior decorators in the seventeenth–eighteenth century in England (Gettens and FitzHugh 1993b) or it was found in the seventeenth century Russian wall paintings (Naumova and Pisareva 1994).

Thermodynamics of basic copper carbonates

Comparing azurite and malachite, the latter is more abundant in nature and is obtained more easily by precipitation. This is in accordance with the thermodynamics. From a thermodynamic point of view, tenorite (CuO) is the most stable solid phase at atmospheric conditions (i.e. partial pressure of carbon dioxide is approximately 40 Pa, corresponding to its common concentration of 0.04% vol. in the air) according to the predominance diagram for the Cu^{2+} – H_2O – CO_2 system (for temperatures 280–350 K) reported by Preis and Gamsjäger (2002). Their values imply that malachite is the most probable product of precipitation at atmospheric conditions, while azurite can form under much higher partial pressure of CO_2 (above 0.1 MPa). Kiseleva et al. (1992) reported values of Gibbs free energy of the transition of malachite to tenorite ($\Delta G_r^\circ = -4.6$ kJ) and the transformation of azurite to malachite ($\Delta G_r^\circ = -28.5$ kJ). These thermodynamic relations mean that the transition of malachite to tenorite is

thermodynamically favourable (i.e. for $\Delta G < 0$ the process proceeds spontaneously), but kinetic factors probably prevent it (i.e. the reaction rate of the transition is very slow). It explains a much wider distribution and more frequent occurrence of malachite relative to azurite in nature and also the fact that azurite commonly alters into malachite.

Basic copper chlorides

Basic copper chlorides (atacamite, paratacamite, clinocatacamite and botallackite, $\text{Cu}_2\text{Cl}(\text{OH})_3$) are well-known corrosion products formed on copper and bronze objects (Scott 2002). Nevertheless, they are also increasingly reported as components of paint layers in various types of painted artworks: panel and easel paintings (Salvadó et al. 2002; Švarcová et al. 2014), as well as wall paintings and polychromed objects (see Table 2). They have been considered to be less common pigments, but some recent studies indicate their regional abundancy, e.g. in the mediaeval murals in Swedish churches, especially on the Gotland island (Nord and Tronner 2018). Yong (2012) reported that in Chinese murals, they were even more popular than green malachite.

Although having identical chemical composition ($\text{Cu}_2\text{Cl}(\text{OH})_3$), the basic copper chlorides differ in crystal structures. Therefore, distinguishing among individual polymorphs is possible only with phase sensitive analysis (such as X-ray powder diffraction, XRPD, or Raman spectroscopy, RS). These pigments of pale vivid green colour exist as natural minerals, which are formed in the weathering zones of copper-bearing ores in arid climates, e.g. in the Atacama Desert (Pollard et al. 1989). Botallackite can form also under influence of seawater as in Botallack mining area in Cornwall, UK (Krause 2006). However, all the minerals are reported as rare, and thus, it can be deduced that their artificial analogues were primarily employed for pigment usage. In fact, there are several mediaeval recipes for preparation of green pigment using common salt (NaCl) or *sal ammoniac* (NH_4Cl). The best known recipe, for *Viride salsum*, was provided by Theophilus in the twelfth century and similar recipes are documented in old Chinese treatises (Scott 2002; Yong, 2012).

Occasionally, other copper chlorides were identified in the paintings: zinc-copper chlorides (Alejandre and Márquez 2006), cumengeite (Švarcová et al. 2009) or calumetite (Naumova and Pisareva 1994; Salvadó et al. 2002). Besides their intentional use, the frequent occurrence of copper chlorides on wall paintings or in the remnants of polychromes on stone or ceramic might also be due to salt corrosion of another copper-based pigment, usually azurite (Švarcová et al. 2009).

Table 2 Notable occurrences of copper chlorides (Cu-Cl) and sulphates (Cu-S)

Date	Artwork	Identified components			Method ^d	Reference
		Type ^a	Cu-Cl ^b	Cu-S ^c		
589–568 BCE	An., Limestone reliefs from the Great Gate, Palace of Apries, Lower Egypt	PS	At?		XRF, FTIR	Hedegaard et al. (2019)
9th c. CE	An., Cave 85 of The Mogao Grottoes, Dunhuang, Gansu Province, China	WP	At		XRPD	Wong and Agnew (2013)
9th c. CE	An., Painted fragment from Tepe Madrasah, Nishapur, northeastern Iran	WP	At		XRPD	Holakooei et al. (2018)
11th c. CE	An., Polychromic sculptures, west wall, Jizo Hall, Chongqing Temple, Shanxi Province, China	PCI	At		RS	Wang et al. (2014)
~1150 CE	An., Byzantine saint, Church in Garde, Gotland, Sweden	WP	At?		SEM/EDS	Nord et al. (2017)
12th c. CE	An., Decorations of fortress on the mount Sofeh in Isfahan, central Iran	WP	At		RS	Holakooei et al. (2020)
12th c. CE	An., Romanesque decoration of the Cathedral Notre-Dame, Tournai, Belgium	WP	At	Pos	RS	Lepot et al. (2006)
~1250	An., Sculptures of Royal Portal of the Cathedral of Bordeaux, France	PS	+ *	Broch*	RS	Daniel et al (2015)
13th c. CE	Cimabue, San Matteo, Upper Basilica in Assisi, Italy	WP	At, Clin*		XRPD	Vagnini et al. (2018)
13th c. CE	An., Decoration of city castle Gozzoburg, Krems, Austria	WP	At, Clin		SR-XRPD	Bidaud et al. (2008)
~1380	Painters at king Charles IV's court, The Joseph's Doubt scene (i); The Adoration of Kings scene (ii), Capitulair hall, Sázava Monastery, Czech Republic	WP	Par, At (i)* At (ii)		XRPD	Švarcová et al. (2009)
13th–15th c. CE	An., Mocarabes, Hall of the Kings, Alhambra, Granada, Spain	PG	Clin*		RS	Domínguez-Vidal et al. (2013)
14th? c. CE	An., Decoration of the Masjid-i Jame of Abarqu mosque, central Iran	WP	At		RS	Holakooei and Karimy (2015)
14th c. CE	Ambrogio Lorenzetti: Madonna and Child Enthroned with Saints, St. Augustine Church, Siena, Italy	WP	Clin*		RS	Damiani et al. (2014)
14th–15th c. CE	An., San Antonio Abate, the church of San Pietro, Quaracchi near Florence, Italy	WP	Pat*		FTIR	Dei et al. (1998)
15th c. CE	An., Southern wall of sedilia, Church of Mother Mary and Fourteen Holy Helpers, Franciscan monastery, Kadaň, Czech Republic	WP	CaI, Cum		XRPD	Švarcová et al. (2012)
15th? c. CE	An., Decoration of chapel of the castle in Ponthoz, Belgium	WP	Clin*		RS	Vandenabeele et al. (2005)
~1520	Parmigianino, St. Giovanni Evangelista Abbey (2nd chapel on the left), Parma, Italy	WP	Broch		RS	Bersani et al. (2003)

Table 2 (continued)

Date	Artwork Author, artwork name, location	Identified components			Method ^d	Reference
		Type ^a	Cu-Cl ^b	Cu-S ^c Other phases/admixtures		
~1520	Michelangelo Anselmi, St. Giovanni Evangelista Abbey (6th chapel on the left), Parma, Italy	WP	Clin*	Malachite	RS	Bersani et al. (2003)
16th c. CE	Master Dionisy, Decoration of the Cathedral of the Nativity of the Virgin, St. Pherapont Monastery, Russia	WP	At	Malachite Pseudomalachite	XRPD	Naumova et al. (1990)
1547 CE	An., Exterior decoration, northern façade, Voronet Monastery, Romania	WP		Dolerophamite (Cu ₂ (SO ₄)O)	RS	Buzgar et al. (2014)
16th c. CE	An., Decoration of the Chapel of Mercy, Arcos de la Frontera, Cádiz, Spain	PS	At, Clin, Zn-Par	Cuprite Gypsum	XRPD	Alejandro and Márquez (2006)
16th c. CE	An., The Adoration of Kings, St. Jacob the Elder Church, Přepeře near Turnov, Czech Republic	WP	Par (i) Cum (ii)	Malachite, gypsum (i)	XRPD	Švarcová et al. (2009)
16th c. CE	An., Exterior St. Paul statue, St. Paul church, Ubeda, Spain	PS	At?	Cu-oxalate?	RS	Campos-Suñol et al. (2009)
16th? c. CE	An., Exterior statues decorating Cathedral in Sevilla, Spain	PS	At*	Azurite	XRPD	Pérez-Rodríguez et al. (1998)
1587 CE	An., Decoration of the church Santa María de Lemoniz Basque Country, Spain	WP		Pos, Ant*	RS	Pérez-Alonso et al. (2006)
1605 CE	An., Gypsum shield on top of a door, Monastery of Santes Creus, Catalonia, Spain	PG	+	Azurite, Cu-oxalates	SR-FTIR	Lluveras et al. (2010b)

^aWP wall painting, P polychromy on stone (S), ceramic (C), gypsum plaster (G), clay (Cl); ^bAt atacamite, Clin clinnoatacamite, Cal calumetite, Cum cumengeite, Par paratacamite; ^cAnt antlerite, Broch brochantite, Pos posnjakite; ^dmethod of identification of Cu-Cl or Cu-S phases: FTIR Fourier transform infrared spectroscopy, SEM/EDS scanning electron microscopy/energy-dispersive spectrometry, SR synchrotron radiation, RS Raman spectroscopy, XRF X-ray fluorescence, XRPD X-ray powder diffraction; *supposed to be corrosion products

Basic copper sulphates

Basic copper sulphates are less-common pigments. They occur in a rather large number of structural polymorphs and have close chemical composition, differing by the number of hydroxyl groups and/or molecules of crystalline water. The most frequently reported basic copper sulphates include brochantite ($\text{Cu}_4\text{SO}_4(\text{OH})_6$) and posnjakite ($\text{Cu}_4\text{SO}_4(\text{OH})_6 \cdot \text{H}_2\text{O}$), less frequently langite ($\text{Cu}_4\text{SO}_4(\text{OH})_6 \cdot 2\text{H}_2\text{O}$) or antlerite ($\text{Cu}_3\text{SO}_4(\text{OH})_4$) (Scott 2002). All of them are formed as secondary minerals in the oxidation zones of copper ores, especially in the arid areas. Similarly to basic copper chlorides, they are relatively rare minerals, usually associated with more abundant malachite.

In the field of cultural heritage, these phases are well-known as corrosion products of copper artefacts exposed to outdoor environments, besides copper chlorides and carbonates, which are also present in the copper patina (Krätchmer et al. 2002). Their occurrence in painted artworks is reported quite sporadically, but they might be present in various types of paintings including illuminated manuscripts (Gilbert et al. 2003), panel and canvas paintings (Naumova et al. 1990; Correia et al. 2007) and/or wall paintings (see Table 2). Their presence is under brisk discussion, since the origin of these pigments remains unresolved. Some authors deduce their artificial origin (Naumova et al. 1990), some explain them as natural impurities of mineral malachite (Bersani et al. 2003), while others describe them as alteration products of another copper pigment (Pérez-Alonso et al. 2006). Obviously, there is no universal explanation of the origin of copper sulphate phases in paint layers, therefore, specific factors have to be considered for the interpretation of their occurrence.

Copper acetates

Copper(II) acetates are the most typical representatives of the so-called verdigris pigments. The term “verdigris” has a loose definition and it does not always refer specifically to copper acetate. It may actually be a mixture of carboxylate salts or even basic copper chlorides, carbonates

or other compounds that resulted from various preparation procedures (Kühn 1993; Scott 2002; Van Eikema Hommes 2004, Kühn 1993). Bluish green or blue verdigris is a typical example of an artificial pigment known since antiquity (Kühn 1993). Its manufacturing consisted in collection of corrosion products formed on the surface of copper and/or copper alloys exhibited to acetic acid vapours as follows from many historical recipes, which advise hanging copper plates in a pot over strong hot vinegar. Since the twelfth century, verdigris of highly regarded quality had been produced in the French wine-growing region around Montpellier as a by-product of the wine-making process (Van Eikema Hommes 2004). Apart from the unrefined verdigris, painters used distilled (also crystallised or purified) verdigris. Distillation was a purification process consisting in dissolution of verdigris in vinegar and subsequent recrystallisation of neutral copper acetate (Kühn 1993; Van Eikema Hommes 2004).

The use of verdigris was confirmed mostly from the thirteenth to the nineteenth century in Europe. It is documented in Gothic panel paintings and illuminations, and was widely used in early oil paintings as a green pigment to produce intense pure green tones for landscapes and draperies (Thompson 1956; Kühn 1993). On the contrary, a conclusive evidence of verdigris in wall paintings is scarce (Villar and Edwards 2005; Damiani et al. 2014; Fioretti et al. 2020), which can reflect both its instability in the conditions of wall painting (Švarcová et al. 2009; Coccato et al. 2017) and the problem with its unambiguous identification.

As it has been already mentioned, there is a nomenclature confusion about the “verdigris” term. Even when using the term verdigris to refer exclusively to copper acetates, the situation does not become much clearer (Table 3). Besides neutral copper acetate, corresponding chemically and structurally to mineral hoganite ($\text{Cu}(\text{CH}_3\text{COO})_2 \cdot \text{H}_2\text{O}$), and its less frequent anhydrous variant, five distinctive basic copper acetates of the general formula $x\text{Cu}(\text{CH}_3\text{COO})_2 \cdot y\text{Cu}(\text{OH})_2 \cdot z\text{H}_2\text{O}$ have been theoretically proposed (Scott 2002). However, the paucity of the reliable crystal structure data has made an exact identification of these substances almost impossible. Recently, the

Table 3 Reported copper acetates of the general formula $x\text{Cu}(\text{CH}_3\text{COO})_2 \cdot y\text{Cu}(\text{OH})_2 \cdot z\text{H}_2\text{O}$

Type	x-y-z phase	Crystal system	Colour	Reference
Neutral (hoganite-like)	1-0-1	Monoclinic	Blue green	Meester et al. (1973)
Neutral (anhydrous)	1-0-0	Triclinic	Blue green	Bette et al. (2019)
Basic	2-1-5	Monoclinic	Pale blue	Bette et al. (2018)
Basic	1-3-2	Monoclinic	Pale green	Švarcová et al. (2011)
Basic	1-2-0	Orthorhombic	Blue	Bette et al. (2017)
Basic	1-1-3	Undetermined	Blue green	Scott (2002)
Basic	1-1-5	Undetermined	Pale blue	Kühn (1993)

crystal structure has been determined for anhydrous neutral copper acetate $\text{Cu}(\text{CH}_3\text{COO})_2$ (Bette et al. 2019) and for basic copper acetates corresponding to the following x - y - z phases—1-3-2 (Švarcová et al. 2011), 1-2-0 and 2-1-5 (Bette et al. 2017, 2018). Nevertheless, other factors (such as the presence of more copper acetate variants, the presence of lead-based pigments, the interactions between copper acetates with organic binders) in the paint layers can impede the successful identification or differentiation of copper acetates (Švarcová et al. 2014).

Copper resinate and other copper organometallics (oleates, proteinates)

Copper resinate is the name commonly given to the transparent green glazes that are coloured by copper salts of resin acids (Kühn 1993). However, the term is often incorrectly used for any green copper-containing glazing paint which does not show discrete pigment particles under the microscope. Such observation is not a positive proof of copper resinate. Colombini et al. (2001) demonstrated that analysis of organic fraction using sensitive method such as gas chromatography and mass spectrometry (GC-MS) is necessary to properly identify copper resinate. The preparation of copper resinate mostly consisted in dissolution of verdigris in a mixture of turpentine (obtained by distillation of natural resin) and turpentine essence under heating. In other ancient recipes, various admixtures such as mastic resin, beeswax, linseed oil or rock alum are found (Kühn 1993; Colombini et al. 2001). However, visually similar paints could be obtained by mixing verdigris with drying oils, mixtures of oils and resins or even proteinaceous media. Nevertheless, Van Eikema Hommes (2004), in agreement with Kühn (1994), pointed out that only oil-based medium was identified in the increasing number of analyses of binding media in copper green glazes carried out in recent years. The transparent copper

green glazes were applied in the easel paintings of the fifteenth to the sixteenth century. They disappeared from artists' palettes in the eighteenth century which is sometimes interpreted as the painters' reaction on recognised colour instability manifested by browning of the green (Van Eikema Hommes 2004; Kühn 1993).

In wall paintings, copper oleates, resinates and/or proteinates seem to be scarce, although some examples have been observed—for example on a mediaeval mural from the Kadaň monastery, Czech Republic (Fig. 3). In some other cases, like in green parts of the Persian oil wall paintings of the Safavid period (1501–1736), there is an uncertainty over whether copper oleates found in the transparent green layers were intentionally prepared or whether they formed spontaneously over time between copper compounds used as pigments and the binding media (Samanian 2015). Examples of copper-proteinate, copper-carbohydrate and/or copper-wax pigments on various Egyptian artefacts are reported by Scott (2016). However, no wall painting was among them.

Origin of copper-based pigments

Identification of the pigment is usually interpreted as the identification of the colour-bearing phase. Such approach is satisfactory for the basic evaluation of the employed palette. However, accompanying phases—such as accessory minerals or remnants of the manufacturing process (Table 2)—can provide additional information relevant for the determination of pigment origin. Consequently, their identification can lead to reconstruction of pigment preparation process or determination of provenance of raw materials. These can both contribute to our understanding of exchange of technological know-how or cultural and economic relations in the past. Therefore, increased attention should be paid to the description of minor accompanying components, which potentially

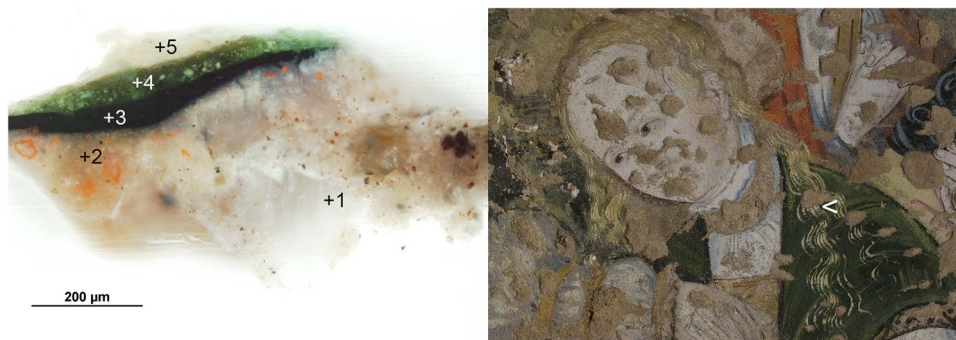


Fig. 3 Copper oleate used in the wall painting in the Franciscan Monastery in Kadaň, Czech Republic, dated to 1520; detail of the painting with the sampling location indicated on the right and cross-section of the micro-sample in visible light on the left; simplified description of

the layer stratigraphy: 1 plaster, 2 oil-based isolation, chalk and minium, 3 charcoal, verdigris, lead-tin yellow, 4 copper oleate (darkening visible on the top)—verdigris, lead-tin yellow and earth pigment, 5 lead white and lead-tin yellow

represent fingerprints of provenance either of the pigments, or the works of art.

Indicators of natural origin

Generally, azurite and malachite are the most abundant natural copper-bearing minerals that were intentionally used as pigments. However, it is always necessary to take into account the local context, as geological situation can differ significantly. For example Tomasini et al. (2013) reported the use of natural atacamite in the colonial polychromed sculpture in Peru, in the neighbouring region of the Atacama Desert, the type locality of atacamite-group minerals. On the other hand, natural origin of atacamite phases detected in paint layers in European context is scarcely conceivable, as there was no available significant and abundant deposit of pure atacamite.

There are two main indicators of natural origin—the size and the morphology of the pigment grains and their characteristic admixtures, which are usually minor and randomly distributed in the paint layer. While homogeneous rounded and mostly small particles (possibly forming aggregates) indicate artificial preparation, mineral grains are usually larger and sharp-edged. Their size varies and can be homogenised only by succeeding grinding. Aru et al. (2014) studied azurite specimens from European and Moroccan copper mining locations with possible relation to medieval mining activities. They identified following mineral phases as common impurities: malachite, hematite (Fe_2O_3), goethite ($\alpha\text{-Fe}^{\text{III}}\text{O}(\text{OH})$), cuprite (Cu_2O), rutile (TiO_2) and anatase (TiO_2), while other minerals such as quartz, calcite, cerussite, orthoclase ($\text{K}(\text{AlSi}_3\text{O}_8)$), beudantite ($\text{PbFe}_3(\text{AsO}_4)(\text{SO}_4)(\text{OH})_6$) and jarosite ($\text{KFe}^{\text{III}}_3(\text{SO}_4)_2(\text{OH})_6$) were less frequent. We can recognise two types of admixtures: (i) very common and non-specific ones, such as Fe oxides, silicates, etc., and (ii) rarer ones that may help specify the mineral's origin and provenance.

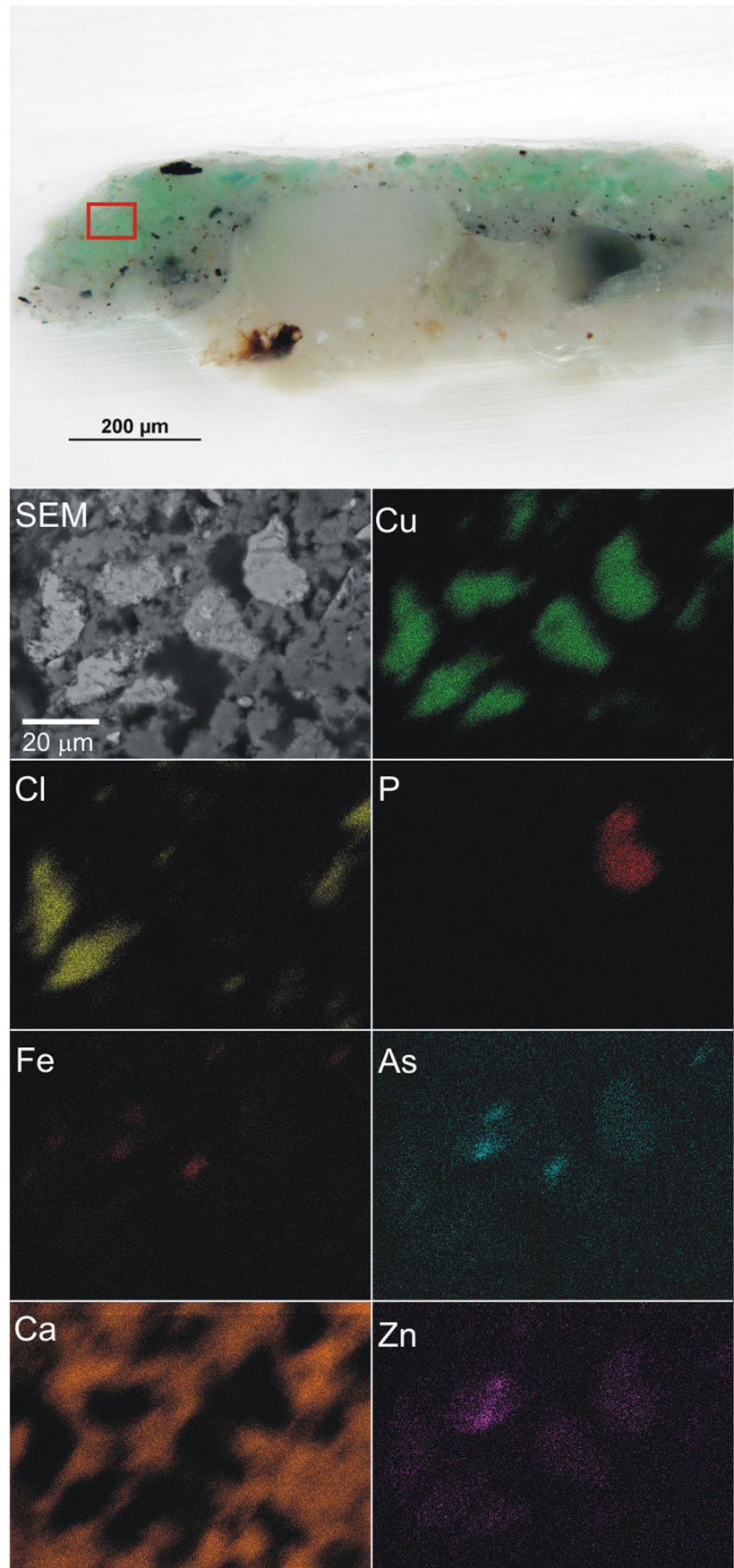
A certain specificity can have, for example admixtures of arsenates (such as olivenite, $\text{Cu}_2(\text{AsO}_4)(\text{OH})$, or adamite, $\text{Zn}_2(\text{AsO}_4)(\text{OH})$) or barium sulphate (barite, BaSO_4). Their presence in natural azurite grains is usually indicated by variable amounts of As and/or Ba. The undoubtedly identification of these minor accompanying minerals depends on their amount and distribution in paint layers. The relatively high concentration of arsenic salts in azurite paint layer from the Gothic Altarpiece in Matejovce, Slovakia, allowed even their detection by micro-XRPD and the position of diffraction lines indicated solid solution of olivenite and adamite type (Hradil et al. 2008). In the Gothic wall paintings in Sázava monastery, Czech Republic (Švarcová et al. 2009), arsenic salts remained intact, while azurite and malachite had partially transformed to atacamite, a corrosion product resulting from chloride action in the masonry. Therefore, they

proved the previous presence of natural pigment (Fig. 4). As and Zn admixtures were found in the azurite and malachite paint layers of wall paintings decorating the cloisters of the bishop castle in Lidzbark Warmiński, Poland, connected culturally with the court of the Holy Roman Emperor Charles IV, whose painters decorated the above-mentioned Sázava monastery (Hradil et al. 2012). Besides copper and zinc arsenates, antimony, nickel, silver and bismuth oxides as well as barite and copper phosphates (pseudomalachite-like minerals) were occasionally found as other minor phases accompanying natural azurite and malachite in the above-mentioned and other paintings (Hradil et al. 2008, 2012; Švarcová et al. 2009, 2012; Bordignon et al. 2008). Copper arsenates were identified also in one of the oldest wall paintings in Ala di Stura, Italy (Aceto et al. 2012), in a green powder in the excavated pot in Pompeii (Aliatis et al. 2019), or in post-Byzantine wall paintings in the Filanthropinon monastery, Greece (Mastrotheodoros et al. 2019), where they detected increased content of Zn and As together with malachite, Ca-Mg inclusions in malachite grains (suggesting the formation of dolomite) and Zn in an azurite paint layer.

These findings bring up a question whether the presence of such admixtures can be useful for tracking back the historic source of the pigments. The presence of arsenic, antimony or silver in copper deposits is reported, e.g. in the Lubietová (Lybethen) deposit located in Banská Bystrica (Neusohl) region, Slovakia (Toegel 2005; Andráš et al. 2010), where the historic mining activity is documented from the thirteenth to the nineteenth century (Heydenreich et al. 2005). Another important copper ore deposit was the French Chessy near Lyon, where the time span of mining was similar, between the thirteenth and the nineteenth century (Gettens and FitzHugh 1993b; Velebil 2008). However, the mining of the oxidation zone (the so-called blue mine) rich in azurite dated to 1811–1845, while in the Middle Ages, the primary sulfidic ore mineralisation (the so-called yellow mine) was probably exploited. The “blue mine” in Chessy locality is predominantly formed by azurite, while malachite, cuprite, smithsonite (ZnCO_3) and barite (BaSO_4) occur only sporadically (Velebil 2008).

The presence of minor phases alone can be understood also as an important material fingerprint, characteristic for an author or a workshop. We can assume that authors associated with individual workshops preferred specific pigment suppliers or sources and that this preference and knowledge of materials was passed on in the community. Buzgar et al. (2014) identified three groups of copper pigments in the exterior wall paintings (all dated to 1547) in the Voronet Monastery, Romania: in addition to azurite, they found malachite associated with conichalcite ($\text{CuCa}(\text{AsO}_4)(\text{OH})$) and basic copper sulphates accompanied by rare dolerophanite ($\text{Cu}_2(\text{SO}_4)\text{O}$). Since the copper sulphates were found only on the north wall and the accessory minerals have different

Fig. 4 X-ray intensity maps of selected elements in the paint layers of the sample from the Gothic wall painting *The Joseph's Doubt*, Sázava Monastery, Czech Republic, indicating the presence of natural minerals accompanying malachite—Cu/Zn arsenates, pseudomalachite (Cu-P), iron oxides—and also secondary Cu chlorides. The analysed area is marked by the red rectangle on the microphotographs of the polished cross-section. Adopted from Švarcová et al. (2012)



genesis (dolerophanite is a volcanic sublimate, while conchalcite forms in the oxidation zone of Cu ores), the authors deduce that either the green copper pigments were obtained from two sources, or that partial repainting could take place on the site.

The above-mentioned examples illustrate that the knowledge of possible accompanying minor phases may help in tracing natural sources of raw materials. In addition, it prevents automatic and simplistic identification of the pigments. A conjoint presence of Cu and As might be, for example erroneously interpreted as emerald green, the presence of Zn as zinc white, mineral barite could be attributed to a later period, being commonly used from the eighteenth century.

Artificial pigments—historical recipes and retrospective syntheses

Principally, there are two ways to reveal the process of a copper pigment's artificial origin. The first one consists in the replication of historical recipes, whose existence, however, do not automatically imply their practical use with a significant impact in the fine art. When replicating various recipes for verdigris, copper greens and azures, numerous authors (Scott 2002; De la Roja et al. 2007; Švarcová 2011) encountered difficulties arising from missing or vague instructions for the reaction conditions, concentrations of ingredients etc. Purification and separation of the required pigment from the by-products and unreacted ingredients is also very frequently neglected.

The second “retrospective” approach interrelates the composition of the pigments found (either as component in paint layers or even as excavated pigment residues) with relevant starting raw materials available in the past and procedures partially documented in the written sources. Such retrospective approach enables to overcome incompleteness in the written instructions and reconstruct (or at least sketch) the way how the pigments could have been produced.

Egyptian blue and green

Although Egyptian blue was used extensively, written sources documenting its manufacture are sporadic. Vitruvius, in the first century BCE, provided the most detailed information about its production (Riederer 1997, pp 27). He described a thorough mixing of finely ground raw materials—sand, flowers of natron and copper sawdust. Subsequently, the conglomerate was formed into balls which were (after drying) put in earthen jars and the jars into an oven (Riederer 1997). There are no details about the time scale or the furnace available. Riederer (1997) pointed out that Vitruvius omitted to mention the source of calcium (e.g. lime), the essential component of Egyptian blue. Evidently, this sophisticated process required good technical ability and

expertise which were passed on from generation to generation very accurately as evidenced by the constancy of the chemical composition of Egyptian blue over 3000 years of its use (Berke 2007).

The nature of Egyptian blue was established in the early nineteenth century, followed by numerous attempts to synthesise it, thus elucidating the basic technological concept: the firing of ingredients introducing copper, silicon and calcium at around 1000 °C, eventually lowered by addition of alkali flux to 900 °C (Riederer 1997). The thorough analysis of the remained pigment cakes excavated in various archaeological sites and numerous retrospective syntheses of Egyptian blue and green provide a good base for deduction of particular aspects of their manufacture and the provenance of the raw materials (Pagès-Camagna and Collinart 2003; Pradell et al. 2006; Shortland 2006; Hatton et al. 2008).

Pagès-Camagna and Collinart (2003) reported substantial differences in the composition of Egyptian blue and green pigment cakes dated to the New Kingdom (1567–1085 BCE). While blue samples contained predominantly cuprorivaite ($\text{CaCuSi}_4\text{O}_{10}$) accompanied by residual silica (quartz and/or tridymite) and silica-rich glass phase, the green samples were characteristic by the presence of parawollastonite (CaSiO_3) together with residual silica (quartz and/or tridymite or cristobalite), both embedded in a silica-rich glass phase. Furthermore, firing residues such as tenorite (CuO) or cassiterite (SnO_2), or, eventually, an unspecified Ca–Si–Sn complex, were occasionally found in the samples of both colours. These findings indicate oxidising conditions (presence of CuO) and the use of bronze scraps (Sn residues) in the production process, which was also evidenced by an extensive set of experiments. They proved that equal proportion of copper and calcium, small addition of flux (below 4%) and the firing temperature between 870 and 1080 °C lead to the ideal Egyptian blue. An accurate Egyptian green required less copper than calcium and more flux, while the firing temperature should be kept between 950 and 1150 °C. Similar proportions of copper and lime for blue and green frits were also indicated by Hatton et al. (2008).

The actual firing temperature can be further distinguished by the presence of various crystal forms of SiO_2 . If only quartz is present, the pigment was fired between 870 and 950 °C. On the other hand, the presence of a high-temperature phases such as tridymite or cristobalite indicates the firing temperature of 950–1100 °C. It has to be taken into account that cristobalite can occur only when the flux concentration is higher than 8%, therefore, it cannot be found in Egyptian blue (Pagès-Camagna and Collinart 2003).

According to Pradell et al. (2006), the cuprorivaite can crystallise and grow within a liquid or glass phase even with an alkali content as low as 0.3% Na_2O . Such a low alkali content results in a low amount of glass phase in the final product and less homogeneous mixture of components.

However, the original amount of glass phase in the samples of ancient Egyptian blue frits cannot always be determined, because of its fast weathering. If the glass is largely degraded and almost missing, its previous presence can be indicated by the abundance and uniform microstructure of cuprorivaite crystals in the pigment frit.

The composition of remnants of a glass phase can be used to suggest the source of alkali flux. Hatton et al. (2008) used the ratio of alkalis $\text{Na}_2\text{O}/\text{K}_2\text{O}$ in the glass phase to differentiate the pigments produced probably using natron (natural evaporite originating mostly from the Wadi Natrun lakes) or plant ashes (derived from salt tolerant coastal and desert plants). Among the investigated samples, plant ashes predominated as indicated by the $\text{Na}_2\text{O}/\text{K}_2\text{O}$ ratio lower than 6, while natron was used as flux only occasionally: in some (not all) green frits exhibiting the $\text{Na}_2\text{O}/\text{K}_2\text{O}$ ratio between 12 and 27.

Furthermore, rounded quartz particles and impurities—like Al_2O_3 (0.3–1.8%) and Fe_2O_3 (0.3–1.3%)—suggest that quartz sand was used rather than crushed pebbles. Lime could be added either as separate component (e.g. crushed limestone or shell) or it could be introduced as a component of the sand: the analysis of sand available in Amarna showed 17% of CaO. The use of lime-rich sand could explain the missing lime in the recipe handed down by Vitruvius. The higher content of MgO (2–6%) in the frits from Zawiyet Umm el-Rakham was tentatively explained by the use of dolomitic limestone. It indicates a parallel existence of more production centres of pigments in Egypt (Hatton et al. 2008).

The composition of metals also varied. The tin was evidenced by Pagés-Camagna and Collinart (2003) and also by Hatton et al. (2008) in Egyptian pigment samples, which indicates the use of 10% tin bronze (according to the observed SnO_2/CuO ratios). However, it was not detected in the samples excavated in Mesopotamia, where copper scraps or copper ore were probably used instead of bronze for the pigment production (Hatton et al., 2008). Ormanci (2020) detected Zn instead of Sn in blue pigment cakes (attributed to Urartian period) from different sites in the region east of Lake Van, Turkey. Zn-enriched Egyptian blue was also detected by Nicola et al. (2019) in the early mediaeval wall paintings in Santa Maria *foris portas* Church in Castelseprio, Italy, and by Vettori et al. (2019) in a contemporary church in southwestern Turkey. It can indicate the use of brass as a local specificity, coming probably from the Byzantine area (Turkey). Moreover, since Zn was present together with minor amounts of lead concentrated in the glassy matrix embedding cuprorivaite grains, the authors speculated about an alternative local technology, which could benefit from the ability of Zn and Pb to act as secondary fluxes. Their intentional use probably permitted to produce Egyptian blue without natron flux in the seventh–ninth century CE, when a general crisis in the supply of natron took place. Application

of lead isotope analysis brings another interesting insight into the provenance of the metals. Shortland (2006), who studied late Bronze Age Egyptian materials (metals, alloys, glasses etc.), pointed out that the source of copper and copper alloys was outside Egypt.

Verdigris

In contrast to Egyptian blue (and related pigments), there are many historical recipes for preparation of verdigris and other copper pigments (Scott 2002). The oldest recipes date back to Pliny's texts from the first century CE (Scott 2002, Chapter 9, pp 279). Similar instructions were given in other early recipes, such as the Latin manuscript known as *Codex Lucensis* (eighth century CE), the miscellaneous collection covering a period from the eighth to the twelfth century known as *Mappae Clavicula* or the twelfth century treatise of Theophilus's *De diversis artibus* (Scott 2002; Orna et al. 1980).

The procedures of copper acetates' production typically consisted in the reaction between metal copper (or its alloy) and acetic acid contained in vinegar fumes. This was achieved, for example by hanging copper plates above hot vinegar in a sealed vessel, which should be stored in a warm place for a certain amount of time. Subsequently, the corrosion product should be scraped from the plates and used directly as a pigment. Particular recipes differ especially in the duration of the product formation. The recommended time ranged from a few days up to 6 months. In addition, different warm places were recorded: hot dung, vine peels, oven, smoke or an ordinary sunny place. Other differences involved the starting materials. Besides urine, which was mentioned as an alternative to vinegar, some recipes advised smearing salt, honey and/or soap onto the copper sheets. In several recipes, copper plates were replaced by brass, or even silver. Mediaeval silver could contain copper as an impurity; pure silver otherwise cannot produce any green or blue corrosion product.

Artificial mineral-type copper pigments

While the artificial origin of verdigris and the way of its production is indisputable, the mediaeval production of mineral-type copper pigments including chlorides, sulphates and carbonates has not been still fully clarified. In wall paintings, these phases can form secondarily, resulting from the degradation of other copper pigments (Table 2). On the other hand, their occurrence in panel and easel paintings, polychromed wooden sculptures or illuminated manuscripts clearly indicates their intentional use (Salvadó et al. 2002; Gilbert et al. 2003; Castro et al. 2008a; Švarcová et al. 2014). The limited natural sources of copper chlorides and

sulphates propound they were also prepared artificially, as suggested in numerous historical recipes.

Recipes for the “salt green”, i.e. copper chlorides, require an addition of common salt (sodium chloride). The best known recipe for *Viride salsum* was recorded by Theophilus in the twelfth century. In his recipe, copper sheets smeared with honey and sprinkled with common salt were placed over hot vinegar in a sealed container and left for 4 weeks in a dung. After that, corrosion products were scrubbed and used as a pigment (Scott 2002). If honey contained reducing saccharides, it gave rise to red cuprite (Cu_2O), turning the resulting pigment brown (Švarcová 2011). Another, and probably more suitable, recipe from *Mappae Clavicula* entitled “Changing copper” recommends to sprinkle vinegar over a mixture of copper fillings with ground salt (in the 4:6 weight ratio) and leave it all for 3 days to turn green (Scott 2002). Similar instructions were mentioned also in various mediaeval Chinese treatises (Yong 2012).

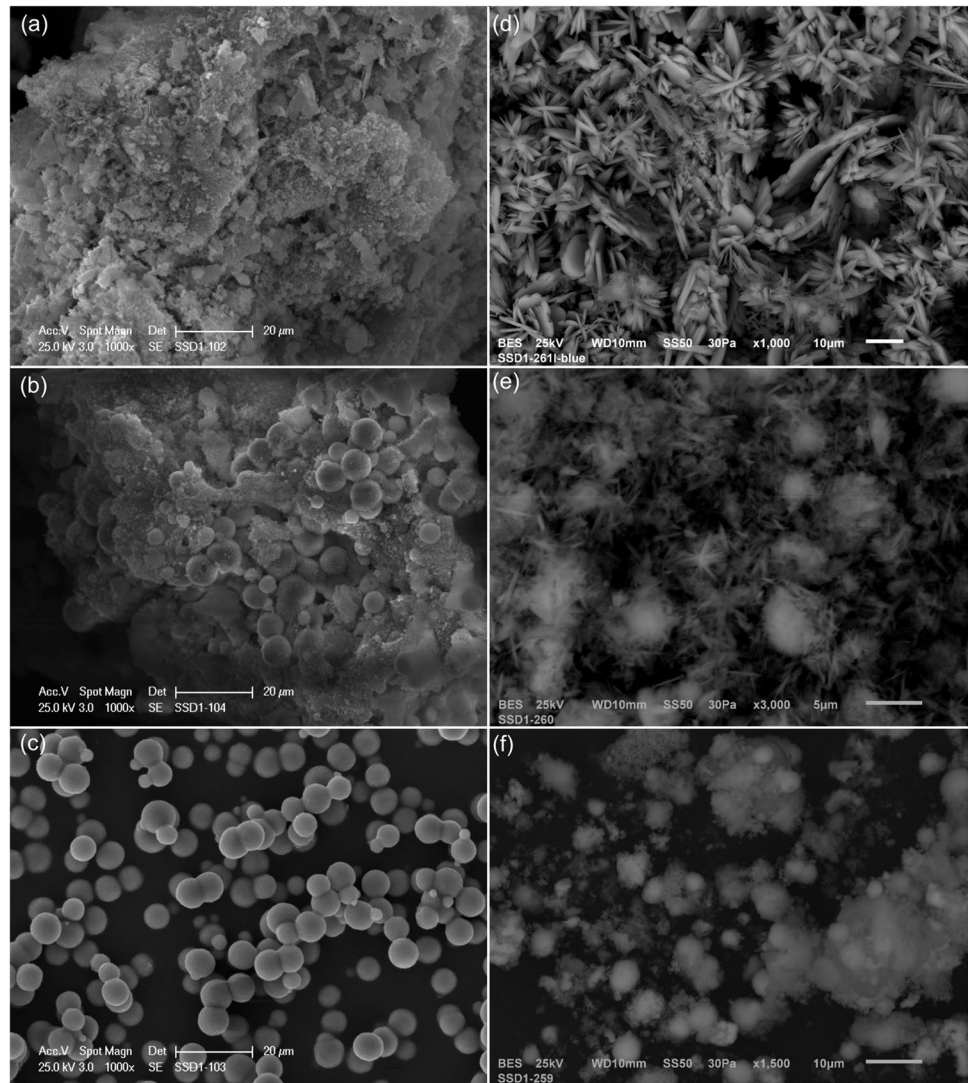
Following the aforementioned recipe from *Mappae Clavicula* (Scott 2002; Švarcová 2011), basic copper chlorides can be easily prepared. Alternatively, they can form together with copper acetates according to the instructions given by Theophilus (Naumova and Pisareva 1994; Scott 2002). In both cases, they are the products of the reaction between metal copper and sodium chloride, promoted by acetic acid. Due to the variable morphology of resulting copper chlorides, it is challenging to identify pigments made with this type of process. However, some clues have been assumed. Salvadó et al. (2002) deduced that the Theophilus's recipe could have been used to prepare green pigments found in the Catalan Gothic altarpieces, as they identified basic copper chlorides together with copper acetate by synchrotron radiation XRPD. Campos-Suñol et al. (2009) surmised the artificial origin of atacamite, as they found associated particles of native copper in the paint layer, suggesting the use of copper fillings for the pigment production. Hedeegard et al. (2019) inferred that Sn-containing atacamite found in some green paint layers on reliefs from the Palace of Apries, Egypt, could be produced using bronze instead of copper. Similar deductions were reported by Alejandro and Márquez (2006), who found copper-zinc hydroxychlorides in green layers covering stone ornaments in a Spanish church. As the natural sources of such minerals are even rarer than those of paratacamite (Braithwaite et al. 2004), the most probable source of such pigment was the corrosion of brass sheets. A modification of the process could take place as suggested by Holakoei et al. (2018) who hypothesised that the occasionally identified atacamite accompanied by minor copper sulphide and calcium phosphate could originate from a copper object corroded in marine environment.

Besides copper chlorides, a variety of pigments can be prepared following the recipes, with addition of more components. A recipe from *Mappae Clavicula* recommends

putting lime with strong vinegar into a copper vessel to produce a different azure, providing probably the so-called lime blue, $\text{CaCu}(\text{OH})_4 \cdot \text{H}_2\text{O}$, which was successfully prepared by Krekel and Polborn (2003). Later recipes (from the twelfth century onward), often entitled “To make a good green or azure”, use verdigris as one of the starting material (Orna et al. 1980; Scott 2002). Other typical raw materials included salt ammoniac, vinegar and/or oil of tartar (saturated solution of K_2CO_3). Other ingredients, such as lime (CaO), potassium alum ($\text{KAl}(\text{SO}_4)_2$), “gesso” (gypsum, $\text{CaSO}_4 \cdot 2\text{H}_2\text{O}$), marble (formed mainly by calcite, CaCO_3) or “cerussa” (lead white) can also appear. The preparation of the pigment usually consisted in mixing and grinding all ingredients together until a soft paste or powder was obtained. After that, it was advised to place it in a tightly closed vessel, which should be placed in some warm place (oven, dung, etc.) for a variable period of time. After some time, the blue or green products were formed. Such recipes are contained, e.g. in a Paduan manuscript *MS 1243* (Italy, fifteenth C), *Manuscript of Bologna* (Italy, fifteenth C), a Paduan manuscript *Riccite per far ogni sorte di colori, MS 992* (Italy, seventeenth C) (Scott 2002; Orna et al. 1980).

Such procedures could provide variable mixtures consisting of different copper chlorides, sulphates and/or malachite (Naumova et al. 1990; Lepot et al. 2006; Švarcová et al. 2009, 2012). However, as already mentioned above, their replications did not lead to satisfactory results. Focusing on the composition of pigments found in paint layers, it is possible to find recipes' ingredients which could have served as reasonable reactants. Among these materials, we can include (i) copper sulphate (blue vitriol) as a source of sulphur and/or copper, (ii) copper acetate (verdigris) as a source of copper, (iii) sodium chloride (salt) and (iv) ammonium chloride (sal ammoniac) as a source of chlorine, (v) sodium carbonate (soda) and (vi) potassium carbonate (potash, oil of tartar) either as a source of carbonate anion or as a base-forming agent. Naumova et al. (1990) demonstrated that the addition of sodium bicarbonate to copper sulphate solution leads to co-precipitation of posnjakite and malachite, which corresponds to similar pigment identified in early sixteenth century Russian wall paintings and in fifteenth century iconostasis. Švarcová et al. (2009, 2011, 2012) altered the reaction conditions by addition of sodium chloride solution, which resulted in various pure or co-precipitated products including posnjakite, brochantite, malachite, atacamite and/or paratacamite. In principle, copper sulphates formed as a first phase, with increasing amount of soda malachite formed. Finally, when the amount of added sodium chloride considerably exceeded stoichiometry, atacamite occurred. The precipitated grains had similar morphology (Fig. 5) as pigments found in paint layers from the sixteenth century wall painting in Přepeře, Czech Republic: malachite with distinct spherulitic shape, irregular or stick-like atacamite

Fig. 5 SEM images of products prepared by precipitation—posnjakite (a), mixture of posnjakite-malachite (b), malachite (c), mixture of posnjakite-brochantite (d), mixture of brochantite-malachite (e) and mixture of malachite-atacamite (f). Adopted from Švarcová et al. (2012)

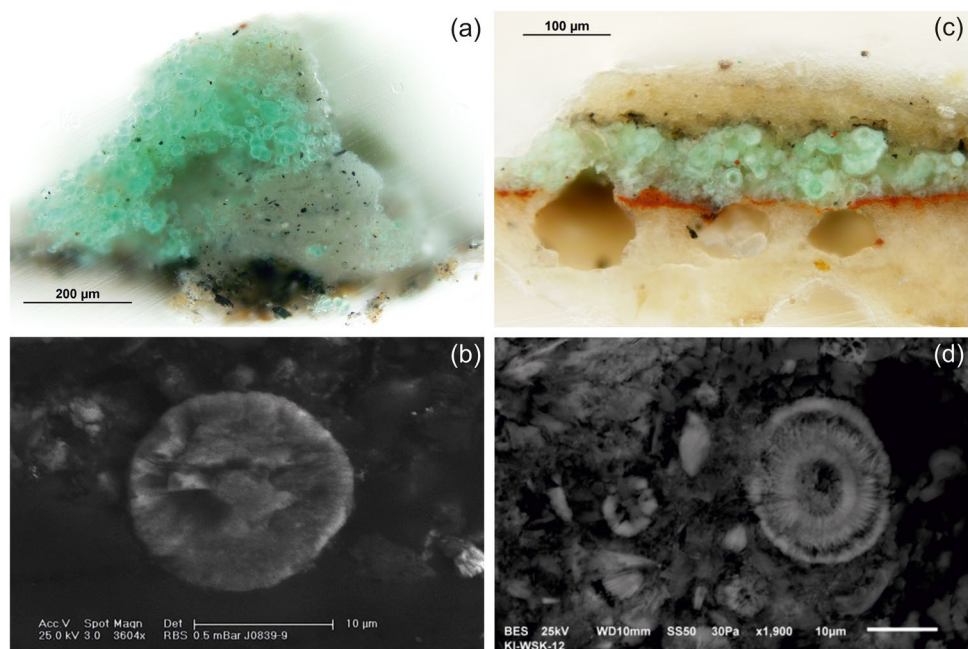


and paratacamite grains and star-shaped conglomerates of posnjakite and brochantite. An interesting feature, connecting various artworks, is the presence of Cu–S–Cl grains. Such grains, typically formed during co-precipitation of basic copper chlorides and sulphates, were found in samples from the wall paintings in Franciscan monastery in Kadaň, Czech Republic (Švarcová et al. 2012) or in polychromed sculptures (Švarcová 2011). However, the association of the phases (Cu carbonates, sulphates and/or chlorides) does not univocally prove their artificial origin. Bersani et al. (2003) explained the presence of brochantite in a Parmigianino’s wall painting as a natural impurity of the employed malachite. Finally, Pérez-Alonso et al. (2006) concluded that copper sulphates found on a Basque wall painting originated from the degradation of malachite.

The explanation of origin of spherulitic malachite requires a special attention. Malachite with distinctive spherulitic grains can be easily prepared by precipitation.

The product is characterised by an almost uniform particle size; in the laboratory tests, the grain size was around 10 μm (Švarcová et al. 2012). However, similar formation of malachite, but under natural conditions, was reported by Heydenreich et al. (2005), who described the natural precipitation of the so-called mountain green (Bergrün) in flowing water from copper mine or on tailings in Cu deposits around Banská Bystrica (Neusohl), Slovakia. The copper ores in this area are predominantly formed by sulphides (tetrahedrite and chalcopyrite). In the presence of water, oxygen and certain bacteria, the sulphides can rapidly oxidise, giving rise to acidic and sulphate-rich water. Subsequently, the copper is leached out into the water. The acid mine drainage is buffered or neutralised by dolomite and calcareous rocks (available in this region) resulting in the precipitation of spherulitic malachite. The pigment was collected once a year, which led to the production of malachite with large particles and strong green

Fig. 6 Comparison of the morphology of artificial (a, b) and naturally precipitated (c, d) spherulitic malachite found in the Gothic wall painting *The Adoration of King*, Sázava Monastery, Czech Republic and in a Gothic wall painting decorating the gallery of the castle in Lidzbark Warmiński, Poland, respectively. Polished cross-sections of the samples in normal reflected light (top); details of the malachite grains in backscattered electrons (bottom). Adopted from Švarcová (2011) and Hradil et al. (2012)



colour. In Fig. 6, there is a comparison of naturally precipitated malachite found in paint layers of Gothic wall painting decorating the cloister of the castle in Lidzbark Warmiński, Poland (Hradil et al. 2012), and artificially precipitated malachite found in one Gothic scene in Sázava monastery, Czech Republic. The artificial origin of spherulitic malachite was supported by the occasional presence of Cu–S–Cl and atacamite grains, which may represent remnants of the precipitation reaction described above (Švarcová et al. 2009).

Besides the above mentioned pigments, a rare pigment, cumengeite, $\text{Pb}_{21}\text{Cu}_{20}\text{Cl}_{42}(\text{OH})_{40}$, was found in a Thailand wall painting (Prasartset 1990) and, later on, in a Bohemian wall painting in Přepeře (Švarcová et al. 2009). In the latter case, the possible formation of cumengeite from corrosion processes was excluded, as no source material of lead was found, and thus, it is highly probable that the use of cumengeite was intentional. The mineral cumengeite is rather rare in nature; it occurs in oxidised zones of lead copper sulphide deposits (Hawthorne and Goat 1986), but its economic exploitation in such purity is hardly possible, thus implying its artificial origin. In addition to the wall paintings in Přepeře, the presence of cumengeite was suggested also in the wall paintings in Kadaň, Czech Republic (Švarcová et al. 2012). However, in this case, cumengeite was present as a minor phase besides the more abundant calumetite, $\text{Cu}(\text{OH},\text{Cl})_2 \cdot 2\text{H}_2\text{O}$ (Fig. 7). The presence of Cu–S–Cl grains suggested formation via precipitation. A possible partial formation of cumengeite was reported also by Bidaud et al. (2008). The precipitation of cumengeite might have been a result of addition of “cerussa” (lead white) in the recipe, another ingredient mentioned in the historical sources.

Degradation of copper-based pigments

Salt attack and oxalic acid

The colour changes of paintings resulting from chemical or structural transformations of the original pigments represent an undesirable process. Regarding the wall paintings, chloride attack is highly presumable under rising or condensing moisture: among the water-soluble salts migrating through masonry and plaster, chlorides belong to the highly soluble and the highly mobile ones and, moreover, their sources are abundant: they are natural constituents of stones and groundwater (Winkler 1994; Moussa et al. 2009), they are present in sea spray in coastal areas (Winkler 1994), they can form from chlorinated water (Dei et al. 1998), they spread from de-icing agents (Winkler 1994) or even common salt that could be added to lime whitewash to enhance the adhesion (Gettens and Stout 1958).

In case of copper-based pigments in wall paintings, polychromed stone or plasterwork artefacts, the changes of blue azurite into green basic copper chlorides and/or malachite represent the most reported degradation type (Gettens and Stout 1958; Bordignon et al. 2008; Kriznar et al. 2008; for others see Table 2). The transitions of malachite to basic copper sulphates or chlorides are recognised to a much lesser extent, probably due to the not-so-pronounced colour change (Vandenabeele et al., 2005; Pérez-Alonso et al. 2006). In certain cases, the identification of the corrosion process is not straightforward, and is facilitated if remnants of the original pigment are preserved and/or if the iconography suggests the use of blue colour (e.g. Virgin Mary’s mantle or sky) (Fig. 8). A detailed microscopic observation of paint layers

Fig. 7 Micro-diffraction patterns of the samples from the wall paintings of the Franciscan Monastery in Kadaň, Czech Republic; identified phases: *C* calcite (CaCO_3), *C** cumengeite ($\text{Pb}_{21}\text{Cu}_{20}\text{Cl}_{42}(\text{OH})_{40}$), *Cl* calumetite ($\text{Cu}(\text{OH},\text{Cl})_2 \cdot 2\text{H}_2\text{O}$), *G* gypsum ($\text{CaSO}_4 \cdot 2\text{H}_2\text{O}$), *L* lead–tin yellow I (Pb_2SnO_4), *M* malachite ($\text{Cu}_2\text{CO}_3(\text{OH})_2$), *P* posnjakite ($\text{Cu}_4\text{SO}_4(\text{OH})_6 \cdot \text{H}_2\text{O}$), *Q* quartz (SiO_2), *W* weddellite ($\text{CaC}_2\text{O}_4 \cdot \text{H}_2\text{O}$), *W** cerussite (PbCO_3); micrographs denote corresponding fragments; ellipses and arrows mark the analysed area and the incident beam direction, respectively. Adopted from Švarcová (2011)

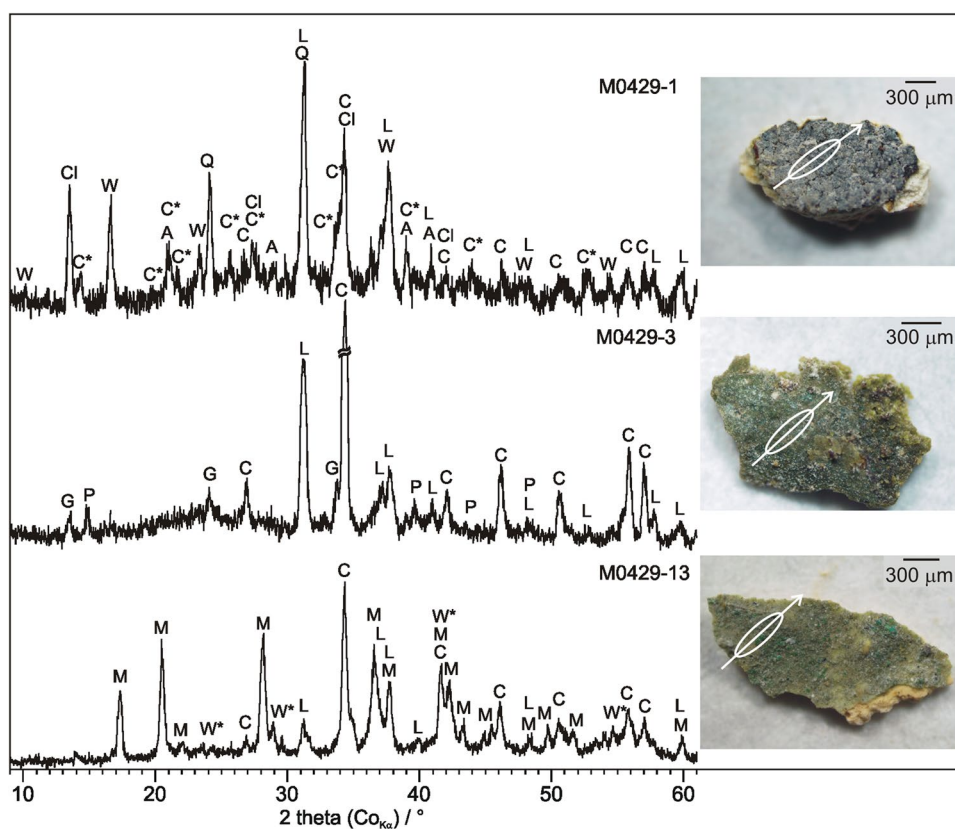


Fig. 8 Photograph illustrating the colour change of Virgin Mary's drapery from blue to green under action of chlorides on the wall painting in the church of Virgin Mary in Mălâncrav, Transylvania, Romania (photo D. Hradil). Adopted from Švarcová et al. (2012)

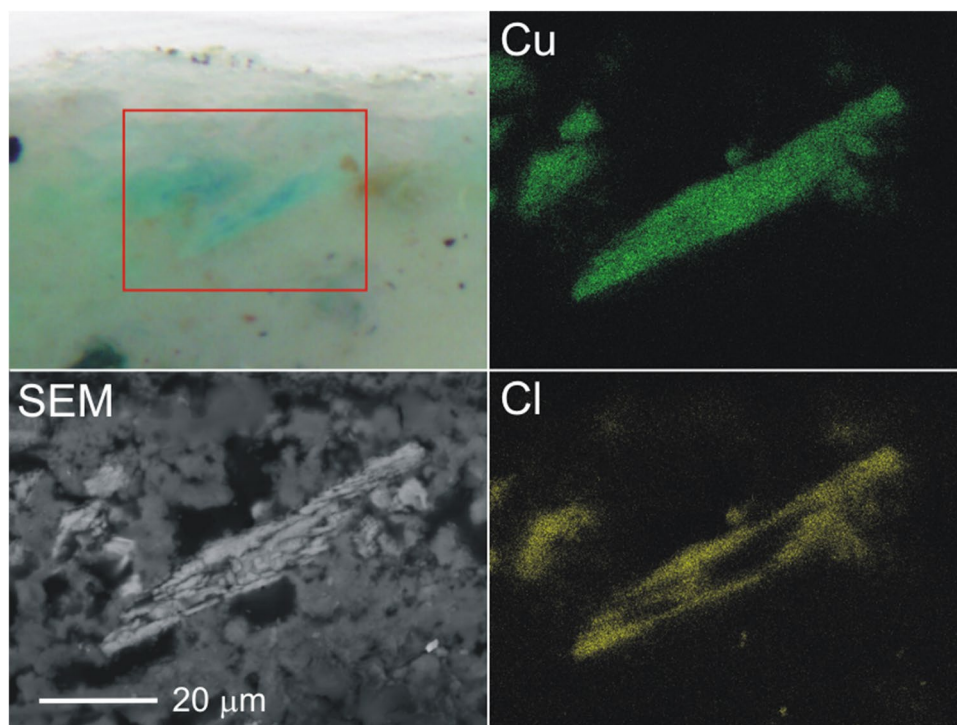
complemented by determination of chemical elements can advance the uncovering of gradual transition of the original copper pigment into a new phase (Fig. 9), to recognise pseudomorphosis after the original grains or to find persisting natural impurities of azurite or malachite (Kriznar et al. 2008; Švarcová et al. 2009; Vagnini et al. 2018). Egyptian blue can also be affected by the chloride-induced corrosion.

This process assumes that the Cu^{2+} ions are firstly leached from the Cu-rich glass phase and then they react with chlorides originating either from the circulating solutions or even from the glass itself. The resulting green atacamite/paratacamite contributes to the change of tonality Schiegel et al. (1989).

Formation of basic copper sulphates from corrosion of another copper pigment is less frequent. Pérez-Alonso et al. (2006) reported transition of malachite to posnjakite and antlerite on a Basque wall painting. In a thermodynamic study, the authors demonstrated that both sulphates can originate from malachite and gypsum, present in the mortar, under action of oxalic acid. Daniel et al. (2015) reported secondary formation of brochantite from azurite in the residual polychrome layers on sculptures decorating the façade of Bordeaux Cathedral, France. Gypsum deposits resulting from atmospheric pollutants (SO_x and dust) are the probable source of sulphates and the reaction was again facilitated by oxalic acid formed by lichens.

Laboratory experiments showed that the resistance against salt attack (NaCl , CaSO_4) decreases in the following order: malachite > azurite > verdigris (Cu acetate) and that the presence of oxalic acid ($\text{H}_2\text{C}_2\text{O}_4$) significantly accelerates the reaction between all the pigments and the salt solutions (Švarcová et al. 2009, 2012). Another experimental study examined the relative reactivity of copper pigments,

Fig. 9 Detail of the paint layer from the Gothic wall painting *The Joseph's Doubt*, Sázava Monastery, Czech Republic, in reflected normal light and back-scattered electrons (left) and corresponding X-ray intensity maps of Cu and Cl indicating the transformation of azurite into copper chloride. Adopted from Švarcová et al. (2012)



gypsum and calcite exposed to oxalic acid solutions of different concentrations (Zoppi et al. 2010). It was shown that verdigris and calcite form copper and calcium oxalates, respectively, already under $0.005 \text{ mol}\cdot\text{l}^{-1} \text{ H}_2\text{C}_2\text{O}_4$ solution (corresponding to pH of ca 2.3), while malachite and gypsum reacted under more concentrated solution ($0.1 \text{ mol}\cdot\text{l}^{-1}$, pH 1.3).

Action of oxalic acid can be easily recognised by the formation of calcium oxalates, weddellite ($\text{CaC}_2\text{O}_4\cdot 2\text{H}_2\text{O}$) and whewellite ($\text{CaC}_2\text{O}_4\cdot \text{H}_2\text{O}$) on the surface of stone artefacts and/or wall paintings. Oxalic acid is either a metabolic product of microorganisms (bacteria, lichens and fungi) living on the artwork's surface, or an oxidation product of degrading organic binders and protective agents applied on the artwork (such as egg, milk, glue, molasses, oils, gum Arabic) (Bordignon et al. 2008; Hradil et al. 2013). Besides the frequently detected calcium oxalates, a copper oxalate that structurally corresponds to a mineral moolooite ($\text{CuC}_2\text{O}_4\cdot n\text{H}_2\text{O}$) was also identified in some paint layers (Bordignon et al. 2008; Castro et al. 2008b; Nevin et al. 2008; Campos-Suñol et al. 2009; Lluveras et al. 2010b; Daniel et al. 2015). In certain cases, copper oxalates were found as the only copper phase and there was no evidence of the original pigments (Castro et al. 2008b; Nevin et al. 2008).

Obviously, the deterioration of copper pigments induced by salts and oxalic acid takes place especially in wall paintings or sculptures exposed to moisture, which enables the transport of salt solutions, the growth of microorganisms and the reactions in the paint layers. A remarkable example

of a synergic effect of all these factors is represented by degradation of pre-Romanesque wall paintings in the St. George church in Kostofany pod Tribečom, Slovakia, where the parts painted by copper pigments became completely discoloured (Hradil et al. 2013) (Fig. 10).

Heat and alkalinity

Exposure of copper pigments to alkalis or heat results in their darkening due to the formation of black tenorite (CuO). Dei et al. (1998) described numerous changes that appeared after conservation of wall paintings of San Antonio Abate in the church of San Pietro at Quaracchi near Florence, Italy, and which consisted in removing gypsum films and efflorescence by saturated solutions of ammonium carbonate and barite hydroxide. This procedure caused transformation of green paratacamite (formed previously as a corrosion product of azurite) into blue copper hydroxide, which transformed both into paratacamite again (when the source of chlorides was not removed) or into black CuO . Alkalinity is an intrinsic property of the lime-based plaster, and thus, the plaster itself represents a potential risk for copper pigments. Mattei et al. (2008) examined the effect of alkalinity in painting substrates, experimentally demonstrating the different behaviour of azurite when applied using fresco and secco techniques. Azurite applied a fresco (lime plaster with pH 12) turned to tenorite during 24 h, while no alteration was observed in the samples applied a secco (lime plaster with pH 8). This problem was probably well-known

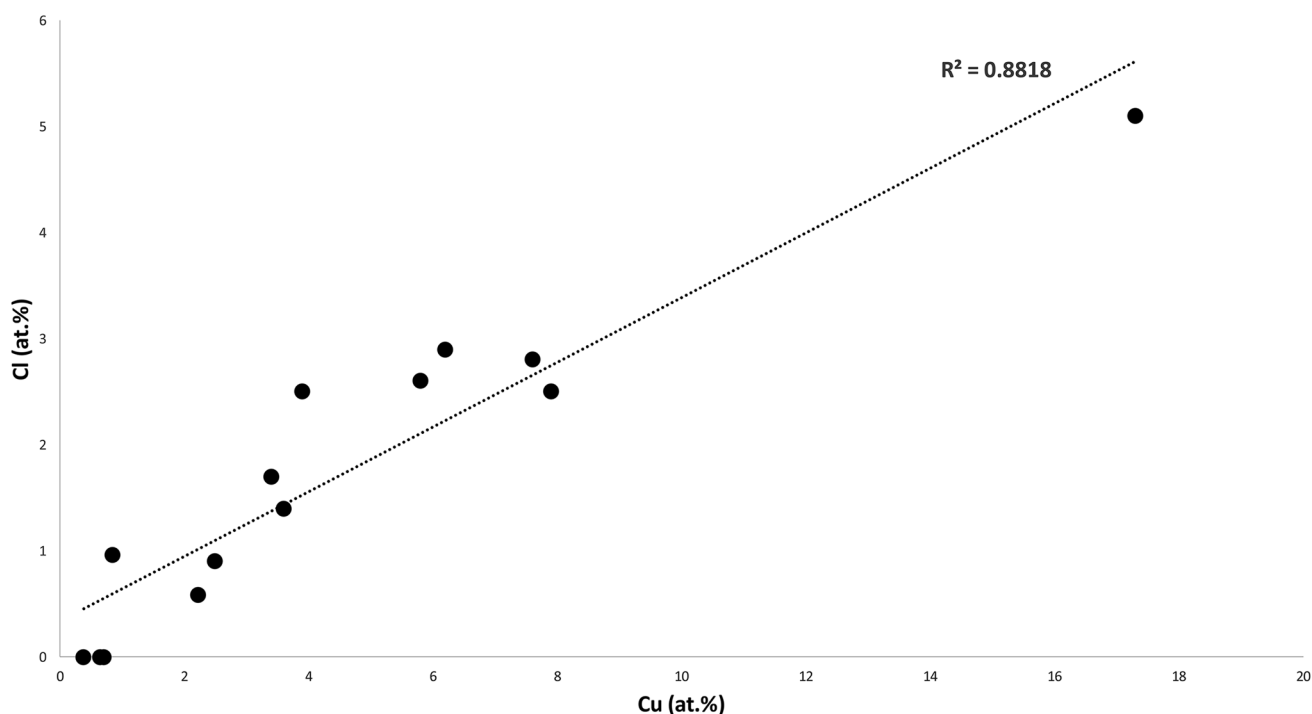


Fig. 10 Correlation of Cu and Cl concentrations based on SEM–EDS measurements of micro-samples from originally blue and green parts (currently not distinguishable by eyes) of pre-Romanesque wall paintings in the St. George’s church in Kostofany pod Tríbečom, Slovakia

to old Masters who applied copper pigments predominantly a secco technique (Thompson 1956). However, additional lime plaster layers covering the original paintings can also be problematic, especially when kept moist before maturing. Investigations of uncovered Gothic wall paintings in the St. Maria-Magdalena church in Bor, West Bohemia, showed that copper pigments darkened completely, although they had been applied on a preparation layer containing gypsum and kaolin. Model experiments proved that kaolinite serves as a good barrier against OH^- anions; however, the moist lime overlayer caused darkening of the tested copper pigments (Švarcová 2011, 2012).

Doménech et al. (2008) reported the conversion of blue azurite to black tenorite on Palomino’s wall paintings in the ceiling of the Sant Joan del Mercat church in Valencia, Spain, as a consequence of fire engulfing the church in 1936. The authors used tenorite content as an indicator of temperature that evolved during the fire in partial parts of the church vault. To a lesser extent, partial blackening can be caused by flame of candles as found, for example by Mugnaini et al. (2006) or Damiani et al. (2014). And finally, heat generated, e.g. by laser or another power source can cause blackening as well. Mattei et al. (2008) studied laser-induced blackening of azurite during analysis by Raman spectrometry. They experimentally determined that the critical grain size for azurite-tenorite conversion was 25 μm and less under the laser power of 3.2 mW.

Alteration of binders, varnishes and glazes

The darkening or the discolouration of paints containing copper pigments is not always a result of pigment degradation, but can be related to alteration of organic materials (Scott 2016; Coccato et al. 2017). Daniels et al. (2004) who studied blackening and brownish-green discolouration of paints containing Egyptian blue concluded that apparent colour changes were caused by surface dirt accumulation, darkening of resin used in varnishes and/or by darkening of aged gum Arabic used as a binder. Cardell et al. (2017) studied ageing of paints consisting of azurite and rabbit glue tempera. They found that the conformational structural changes in binders are responsible for colour changes to green and yellow hues and that these changes are more remarkable in paints with fine-grade azurite, suggesting pigment-binder interactions. Odlyha et al. (2000) investigated chemical changes in model paints with azurite and egg tempera for usage as chemical dosimeters. On the one hand, azurite improved the photostabilisation of the tempera; on the other hand, the pigment-binder interactions lowered the thermal stability of the pigment. Finally, when exposed to NO_x/SO_x pollutants, neo-formed nitrates/nitrites and sulphates were detected on the surface of the paint. Darkening (most likely browning or blackening) is frequently documented process of degradation of Cu-containing glazes based on oils, resins, and also proteins.

Analytical methods: good practises

The chemical and structural diversity of colour-bearing phases together with a variety of accompanying phases forming copper-based greens and blues usually requires employment of several complementing methods and, ideally, combination of in situ analysis with a thorough laboratory investigation of micro-samples (Brunetti et al. 2016; Costantini et al. 2018).

Generally, the materials research can be divided into two parts: screening and subsequent targeted analysis. The key difference is that while the screening looks for questions, the targeted analysis answers them. Screening should therefore be fast and non-invasive. Conversely, targeted analysis often needs to be invasive (e.g. requires sampling) and detailed, because otherwise it will not answer the question. The most common mistake of materials research of works of art is that screening is neglected and questions are not asked correctly. As a result, a large number of samples is taken and analysed, and instead of targeted analysis, only very expensive and invasive screening is additionally performed.

Step 1: screening of Cu contents

Visual inspection of an artwork accompanied by common methods of restorer's research (e.g. IR reflectography, X-ray radiography) are usually not sufficient for recognition of the presence/spatial distribution of Cu pigments, partially due to their frequent degradation and loss of original colour. In addition to the most typical green and blue shades, Cu pigments can also be present in black (due to blackening or thinning/transparency of the colour layer and visibility of a black underpainting) or brown (due to the degradation of glaze layers). In highly degraded murals, Cu pigments may be residually present even in completely discoloured parts of the painting (Hradil et al. 2013).

The best method for the detection of low Cu contents in situ is X-ray fluorescence (XRF). When screening wall paintings, hand-held XRF analysers are advantageous, enabling to perform measurements even in hard-to-reach places, on scaffolding, etc. The advantage of elemental analysis using X-ray fluorescence is its high sensitivity to heavy elements in light matrix. Therefore, concentration of Cu in hundreds or even tens of ppm can be detected in the plaster (Cihla et al. 2017). In addition, the presence of copper is almost exclusively related to the use of Cu pigments, as other sources of Cu (atmosphere, humidity) can generally be ruled out. It may happen that some types of sand used for the production of plaster may contain

some natural admixtures of Cu-containing phases—in this case, however, Cu will be homogeneously distributed in the whole area of the wall painting, and not correlated with individual scenes or parts of the painting. In most cases, of course, the concentration of Cu originating from pigments will be significantly higher.

The spatial distribution of Egyptian blue as well as Han blue and purple can be alternatively mapped by recording their visible-induced luminescence even if their traces—undetectable by naked eye—remain (Verri 2009; Gasanova et al. 2018; Asscher et al., 2019).

Step 2: interpretation of minor admixtures (if possible)

Only in some cases, non-invasive XRF screening can provide more detailed information on the nature of the employed Cu pigments—e.g. distinguishing chemical compounds or proving their natural origin. The main complicating factors are the following: (i) it may not be clear whether the detected Cu comes from the original painting layer (for more complicated stratigraphy of paint layers, portable XRF is generally an insufficient method); (ii) the detected S and Cl contents can also be associated with other elements, particularly calcium, and not exclusively with copper; and (iii) it is necessary to take into account the limited detection range when measuring in air (particularly for light elements) and also lower spectral resolution leading to misinterpretation of overlapping lines (e.g. Pb vs. S).

On the other hand, if the stratigraphy is simple, the layer is homogeneous and the Cu pigment concentration is high, the XRF technique is sensitive enough to detect even minor impurities, such as As, Zn or Ba in azurite, which can prove its natural origin (Hradil et al. 2008). However, it is always necessary to exclude other possible sources (e.g. an admixture of Ba or Zn white in the mixture), which can be very difficult with only non-invasive tools. If the stratigraphy is simple and the artwork is also easily transportable, the range of possible non-invasive analytical and imaging methods expands significantly. Smieska et al. (2017) mapped impurities in azurite found in an illuminated manuscript by synchrotron-based high-energy X-ray fluorescence mapping (SR-XRF) and diffraction mapping (SR-XPRD). However, an access to synchrotron-based analytical techniques is only possible on the basis of submitted and approved research project.

Step 3: planning targeted analysis

The results of non-invasive screening will allow to decide whether the artwork should be studied in more detail. From the viewpoint of restoration/conservation, a detailed study is always appropriate when degradation and colour changes are

evident, and also whenever it is necessary to investigate the painting technique or issues related to historic or regional attribution. If sampling is not allowed, useful information can be alternatively obtained by portable spectroscopic methods (see step 5).

Step 4: microscopic observation and detailed elemental analysis

Light microscopy (LM) is commonly used for basic examination of collected micro-samples and their cross-sections in visible and UV light. Cu pigments are usually indicated by blue and green shades and almost no luminescence in UV light. Scanning electron microscope (SEM) in combination with LM is used to describe the morphology and size of the grains. As described in previous sections, these parameters are often important in assessing the origin of the pigment. Simultaneously with the morphological analysis, it is necessary to perform detailed measurements of elemental composition, most often using an energy-dispersive spectrometer integrated in scanning electron microscopes (SEM–EDS). Compared to laboratory micro X-ray fluorescence (micro-EDXRF), SEM–EDS exhibits better spatial resolution allowing detailed investigation of individual grains: including identification of natural impurities in mineral pigments (particularly As, Zn, Sb or Ba) and spatial distribution mapping of elements (e.g. Cu, S, Cl) in selected areas, which is particularly important for the description of degradation processes. Other methods of elemental microanalysis are much less frequent. Although the interest in laser-based techniques—like laser-induced breakdown spectroscopy (LIBS) or laser ablation-inductively coupled plasma-mass spectrometry (LA-ICP-MS)—is systematically increasing in archaeometry and cultural heritage research, they are still used only rarely for differentiating pigments in paints or for their provenance analysis. Syta et al. (2018) have tested the LIBS/ICP-MS tandem instrument to analyse paint cross-sections and perform an elemental mapping in order to differentiate Egyptian blue and ultramarine pigments. Wagner et al. (2019) compared the quantification of the main elements obtained by SEM–EDS and LA-ICP-MS methods for selected pigments, including also emerald green. It should also be mentioned that both LIBS and LA-ICP-MS are micro-destructive. In addition, the elemental analysis cannot be directly linked to morphological analysis.

Step 5: FTIR and Raman micro-spectroscopy

Both Fourier transform infrared (FTIR) and Raman spectroscopy (RS) belong to the traditional and widespread spectroscopic methods in the field of cultural heritage analysis (e.g. Lauwers et al. 2014; Brunetti et al. 2016), which further include fibre optic reflectance spectroscopy (FORS) and

other related methods (Gasanova et al. 2018; Asscher et al., 2019). With high spatial resolution, FTIR micro-spectroscopy (micro-FTIR) can directly distinguish the basic groups of copper pigments in micro-samples: carbonates, acetates, sulphates, chlorides (Švarcová et al. 2014), and also modern As-containing (emerald and Scheele's) greens (Herm 2020). However, in case of complicated mixtures, numerous overlaps of characteristic lines can represent a complicating factor. Since FTIR is the most suitable method of non-destructive microanalysis of organic binders, an interpretation of the painting technique can be performed together with the identification of Cu pigments. As already mentioned, Cu pigments were applied *asecco* on wall paintings and they were usually mixed with organic binder. However, due to extensive degradation, the residues of the binder are often below the detection limit of FTIR, which implies the use of micro-destructive methods (e.g. chromatographic or mass-spectroscopic techniques), or the painting technique has to be interpreted just on the basis of indirect evidence (e.g. the presence of oxalates). If possible, it is advantageous to employ attenuated total reflection (ATR) FTIR measurement, as it avoids deformations of spectra, which are otherwise very common in contactless reflection mode (Prati et al. 2016).

RS is a suitable method for direct identification of mineral types of copper pigments: the characteristic lines of azurite, malachite, brochantite, Egyptian blue, chrysocolla and others are well-documented. In addition, RS was used to differentiate emerald and Scheele's green (Herm 2020), verdigris or even copper resins (Conti et al. 2014). However, RS has certain limiting factors that have to be taken into account. For example in the identification of green and blue pigments, the choice of laser wavelength plays a key role—significantly better results were achieved with an excitation wavelength of 532 nm than with 785 nm (Marcaida et al. 2018). Even with suitable excitation wavelength, the analyses of actual paintings can often be hindered by fluorescence, and (unlike XRPD, see step 6) RS does not permit to perform quantitative analysis. This can be challenging during interpretation, as the intensities of peaks are not proportional to the concentration of individual compounds in the mixture, they rather indicate how strongly each particular pigment scatters the incoming radiation. Therefore, among the strongly scattering pigments (typically simple oxides or sulphides like hematite or cinnabar), pigments exhibiting poor Raman scattering can be identified only with difficulties (although they may predominate in the mixture) (Košťářová et al. 2013). Nevertheless, especially the analysis of individual grains in the paint layer—made possible by spatial resolution of Raman microscopes—can provide interesting and important results.

FTIR and RS can be performed also *in situ*, either with hand-held instruments or small benchtop spectrometers

equipped with fibre optics and a measuring probe. These are advantageous especially when no sampling of the artwork is permitted. However, one must take into account that due to the low penetration of IR radiation, only upper layers of paintings can be analysed by FTIR, which is usually problematic when varnish is applied on the artwork (on easel paintings) or they were secondarily impregnated. During analysis with portable Raman spectrometers, one must very carefully set the laser power. Higher power can increase the desired signal/noise ratio, nonetheless, especially in the dark and highly-absorbing parts of the paint, the RS analysis may be microdestructive (Mattei et al. 2008), which is unacceptable especially when analysing highly precious works of art.

Step 6: X-ray powder micro-diffraction (micro-XRPD)

XRPD is a key method in solving questions of the origin of Cu pigments, the reconstruction of their possible production procedure and also in the study of their degradation processes. It is the only method of direct phase analysis which can offer quantitative data even when studying micro-samples. To perform the analysis in micro-diffraction mode (micro-XRPD), laboratory diffractometers have to be equipped with monocapillary or polycapillary optics collimating the primary X-ray beam to selected area of the size varying from one to several hundred micrometres (Švarcová et al. 2010). Compared to RS, XRPD has worse spatial resolution and longer acquisition times (most typically in hours). However, if high spatial resolution is not required, the amount of information obtained by XRPD largely exceeds the one obtained by RS: it is possible to directly obtain relatively robust information about all major crystalline phases, their relative proportions, particle sizes and crystallinity (Fig. 7). Therefore, XRPD is better suited for direct phase microanalysis of an unknown sample than RS, and complementary use of FTIR and XRPD may be more effective than a combination of FTIR and RS (Švarcová et al., 2014). Švarcová et al. (2009) showed that micro-XRPD analysis of fragments of mediaeval murals can readily distinguish the original natural pigments (such as azurite, malachite), artificial pigments (such as cumengeite, posnjakite, spherulitic malachite) and also the products of their degradation (such as atacamite, paratacamite). In addition, neo-formed secondary phases on the surface of the paintings (such as oxalates) usually provide intense diffraction lines, which facilitate their identification by XRPD. In comparison with FTIR and RS, the portable XRPD systems are not commonly available for in situ analysis. An example of successfully combined XRF and XRPD systems for in situ analysis of

Egyptian wall paintings was reported by Pagè-Camagna et al. (2010).

Step 7: advanced techniques

Recently appearing hybrid analysers, comprising Raman spectroscopy, scanning electron microscopy and/or energy-dispersive spectrometry, seem to be promising tools for the investigation of multi-layered painting systems (Guerra and Cardell 2015; Wille et al. 2018). These techniques allow 3D morphological studies together with elemental, molecular, structural and electronic analyses of a single complex micro-sized sample. However, more analyses performed on samples from real artworks are necessary to evaluate their real benefits for conservation science.

In case of specific interest in structures, properties, production pathways or degradation processes, it may be required to use special analytical techniques. Such study was performed, e.g. by Pagès-Camagna et al. (2006), who employed synchrotron-based methods to analyse local chemical environment of Cu^{2+} in archaeological Egyptian blue and modern Egyptian green by X-ray absorption near-edge structure (XANES) and extended X-ray absorption fine structure (EXAFS) in order to understand the colouring mechanisms in both of these pigments.

Conclusions

The group of copper pigments is diverse, which is related to the intense colouration of various Cu-containing compounds. Their colour encompasses blue and green as well as a number of transitional shades like turquoise. The pigments were either manufactured, which commonly resulted into complex products (e.g. Egyptian blue and green, Chinese blue and purple) or copper salts or their diverse mixtures (e.g. carbonates, sulphates and/or chlorides; variable copper acetates), or were extracted from natural sources (e.g. azurite and malachite).

The different chemical character of the copper pigments is reflected by significant differences in their stability and durability. While ancient artificially prepared pigments (Egyptian blue, Han blue) are very stable silicates, later more common carbonates (azurite), sulphates (brochantite) or chlorides (atacamite) are often subject to corrosion due to various external conditions. In murals, the most common causes of degradation are dissolved salts migrating in pores and the alkaline environment. There are well-documented processes, such as transition of blue azurite to green malachite or atacamite, and it may not always be entirely clear which mineral phases were original and which were formed secondarily.

The analysis of Cu-compounds requires a multi-analytical approach, including light microscopy, SEM–EDS, XRPD and/or vibrational spectroscopies. It is highly desirable to combine in situ screening and following targeted laboratory analysis of micro-samples. Such approach leads to correct identification of even very unusual phases like cumengeite or calumetite. It is probable that the list is not complete and other interesting Cu phases will be discovered in the future. In numerous cases, only a good knowledge of the context helps to decide if the pigment is original or resulting from degradation.

Copper pigments have been used throughout the history of painting and they still present unexplored areas regarding their nature, manufacturing processes or linking with actual historical mining sources. The space is open for further research.

Acknowledgements The authors acknowledge all cooperating restorers with thanks.

Funding The study was supported by the Academy of Sciences of the Czech Republic within the programme Strategy AV21 No. 23—City as a Laboratory of Change; Construction, Historical Heritage and Place for Safe and Quality Life.

Data Availability Data sharing is not applicable to this article as no new data were created or analysed in this study.

Code availability. Not applicable.

Declarations

Conflict of interest The authors declare no competing interests.

References

- Aceto M, Gatti G, Agostino A, Fenoglio G, Giordano V, Varetto M, Castagneri G (2012) The mural paintings of Ala di Stura (Piedmont, Italy): a hidden treasure investigated. *J Raman Spectrosc* 43:1754–1760. <https://doi.org/10.1002/jrs.4066>
- Aceto M (2021) The palette of organic colourants in wall paintings. *Archaeol Anthropol Sci*. <https://doi.org/10.1007/s12520-021-01392-3>
- Alejandre FJ, Márquez G (2006) Copper-zinc hydroxylchlorides: origin and occurrence as paint pigments in Arcos de la Frontera's chapel of Mercy (Spain). *Eur J Mineral* 18:403–409. <https://doi.org/10.1127/0935-1221/2006/0018-0403>
- Aliatis I, Bersani D, Campani E, Casoli A, Lottici PP, Mantovan S, Marino IG, Ospitali F (2019) Green pigments of the Pompeian artists' palette. *Spectrochim Acta A* 73:532–538. <https://doi.org/10.1016/j.saa.2008.11.009>
- Andráš P, Dirner V, Ladomerský J, Horňáková A (2010) Toxicity of arsenic and antimony in the area of Cu-Ag deposit Lubietová. *Mineralia Slovaca* 42:279–286. https://www.geology.sk/wp-content/uploads/2019/10/MS_3_10_01_Andras_et_al.pdf
- Arizzi A, Cultrone G (2021) Mortars and plasters – how to characterise hydraulic mortars. *Archaeol Anthropol Sci*. <https://doi.org/10.1007/s12520-021-01404-2>
- Aru M, Burgio L, Rumsey MS (2014) Mineral impurities in azurite pigments: artistic or natural selection? *J Raman Spectrosc* 45:1013–1018. <https://doi.org/10.1002/jrs.4469>
- Asscher Y, Angelini I, Secco M, Parisatto M, Chaban A, Deiana R, Artioli G (2019) Combining multispectral images with X-ray fluorescence to quantify the distribution of pigments in the frigidarium of the Sarno Baths, Pompeii. *J Cul Her* 40:317–323. <https://doi.org/10.1016/j.culher.2019.04.014>
- Becker H (2021) Pigment nomenclature in the ancient Near East, Greece, and Rome. *Archaeol Anthropol Sci*. <https://doi.org/10.1007/s12520-021-01394-1>
- Berke H (2007) The invention of blue and purple pigments in ancient times. *Chem Soc Rev* 36:15–30. <https://doi.org/10.1039/B606268G>
- Bersani D, Antonioli G, Lottici PP, Casoli A (2003) Raman microspectrometric investigation of wall paintings in S. Giovanni Evangelista Abbey in Parma: a comparison between two artists of the 16th century. *Spectrochim Acta A* 59:2409–2417. [https://doi.org/10.1016/S1386-1425\(03\)00081-7](https://doi.org/10.1016/S1386-1425(03)00081-7)
- Bette S, Kremer RK, Eggert G, Tang CC, Dinnebier RE (2017) On verdigris, part I: synthesis, crystal structure solution and characterisation of the 1–2–0 phase $(\text{Cu}_3(\text{CH}_3\text{COO})_2(\text{OH})_4)$. *Dalton Trans* 46:14847–14858. <https://doi.org/10.1039/c7dt03288a>
- Bette S, Kremer RK, Eggert G, Dinnebier RE (2018) On verdigris, part II: synthesis of the 2–1–5 phase, $\text{Cu}_3(\text{CH}_3\text{COO})_4(\text{OH})_2 \cdot 5\text{H}_2\text{O}$, by long-term crystallisation from aqueous solution at room temperature. *Dalton Trans* 47:8209–8221. <https://doi.org/10.1039/c8dt01758a>
- Bette S, Costes A, Kremer RK, Eggert G, Tang CC, Dinnebier RE (2019) On verdigris, part III: crystal structure, magnetic and spectral properties of anhydrous copper(II) acetate, a paddle wheel chain. *Z Anorg Allg Chem* 645:988–997. <https://doi.org/10.1002/zaac.201900125>
- Bidaud E, Halwax E, Pantis E, Sipek B (2008) Analyses of a green copper pigment used in a thirteenth-century wall painting. *Stud Conserv* 53:81–92
- Bordignon F, Postorino P, Dore P, Laurenzi Tabasso M (2008) The formation of metal oxalates in the painted layers of a medieval polychrome on stone, as revealed by micro-Raman spectroscopy. *Stud Conserv* 53:158–169
- Braithwaite RSW, Mereiter K, Paar WH, Clark AM (2004) Herbertsmithite, $\text{Cu}_3\text{Zn}(\text{OH})_6\text{Cl}_2$, a new species, and the definition of paratacamite. *Mineral Mag* 68:527–539. <https://doi.org/10.1180/0026461046830204>
- Bredal-Jørgensen J, Sanyova J, Rask V, Sargent ML, Therkildsen RH (2011) Striking presence of Egyptian blue in a painting of 1524. *Anal Bioanal Chem* 404:1433–14399. <https://doi.org/10.1007/s00216-011-5140-y>
- Brunetti B, Miliani C, Rosi F, Doherty B, Monico L, Romani A, Sgamellotti A (2016) Non-invasive investigations of paintings by portable instrumentation: the MOLAB experience. *Top Curr Chem* (z) 374:10. <https://doi.org/10.1007/s41061-015-0008-9>
- Burgio L (2021) Pigments, dyes and inks – their analysis on manuscripts, scrolls and papyri. *Archaeol Anthropol Sci*. <https://doi.org/10.1007/s12520-021-01403-3>
- Buzgar N, Buzatu A, Apopeia AI, Cotiuğă V (2014) In situ Raman spectroscopy at the Voronet, Monastery (16th century, Romania): new results for green and blue pigments. *Vib Spectrosc* 72:142–148. <https://doi.org/10.1016/j.vibspec.2014.03.008>
- Campos-Suñol MJ, De la Torre-Lopez MJ, Ayora-Cañada MJ, Dominguez-Vidal A (2009) Analytical study of polychromy on exterior sculpted stone. *J Raman Spectrosc* 40:2104–2110. <https://doi.org/10.1002/jrs.2379>
- Çamurcuoğlu DS (2015) The wall paintings of Çatalhöyük (Turkey): materials, technologies and artists. Dissertation, University College London, UK. <http://discovery.ucl.ac.uk/1471163/1/>

- [Camurcuoglu_compressed.pdf.%20COMPLETE.pdf](#) (accessed on 7 November 2020)
- Cardell C, Herrera A, Guerra I, Navas N, Simón LR, Elert K (2017) Pigment-size effect on the physico-chemical behavior of azurite tempera dosimeters upon natural and accelerated photo aging. *Dyes Pigments* 141:53–65. <https://doi.org/10.1016/j.dyepig.2017.02.001>
- Caroselli M, Ruffolo SA, Piqué F (2021) Mortars and plasters – how to manage mortars and plasters conservation. *Archaeol Anthropol Sci*. <https://doi.org/10.1007/s12520-021-01409-x>
- Castro K, Pessanha S, Proietti N, Princi E, Capitani D, Carvalho ML, Madariaga JM (2008a) Noninvasive and nondestructive NMR, Raman and XRF analysis of a Blaeu coloured map from the seventeenth century. *Anal Bioanal Chem* 391:433–441. <https://doi.org/10.1007/s00216-008-2001-4>
- Castro K, Sarmiento A, Maguregui M, Martínez-Arkarazo I, Etxebarria N, Anguo M, Barrutia MU, González-Cembellín JM, Madariaga JM (2008b) Multianalytical approach to the analysis of English polychromed alabaster sculptures: μ Raman, μ EDXRF, and FTIR spectroscopies. *Anal Bioanal Chem* 392:755–763. <https://doi.org/10.1007/s00216-008-2317-0>
- Cavallo G, Aceto M, Emmenegger R, Keller AT, Lenz R, Villa L, Wörz S, Cassitti P (2020) Preliminary non-invasive study of Carolingian pigments in the churches of St John at Müstair and St Benedict at Malles *Archaeol. Anthropol Sci* 12:73. <https://doi.org/10.1007/s12520-020-01024-2>
- Cavallo G, Riccardi MP (2021) Glass-based pigments in painting. *Archaeological and Anthropological Sciences*. (forthcoming)
- Cihla M, Trefný M, Drda P, Hradil D, Hradilová J (2017) Non-invasive material and traceological research of the stone head from Celtic settlement Závist near Prague. Proceedings of the 6th interdisciplinary ALMA conference, Brno, Czech Republic, June 1–3, 2017 - *Acta Artis Academica* 2017, 141–149.
- Coccatto A, Moens L, Vandenabeele P (2017) On the stability of mediaeval inorganic pigments: a literature review of the effect of climate, material selection, biological activity, analysis and conservation treatments. *Herit Sci* 5:12. <https://doi.org/10.1186/s40494-017-0125-6>
- Colombini MP, Lanterna G, Mairani A, Matteini M, Modugno F, Rizzi M (2001) Copper resinate: preparation, characterisation and study of degradation. *Ann Chim* 91:749–757
- Conti C, Striova J, Aliatis I, Possenti E, Massonnet G, Muehlethaler C, Polie T, Positano M (2014) The detection of copper resinate pigment in works of art: contribution from Raman spectroscopy. *J Raman Spectrosc* 45:1186–1196. <https://doi.org/10.1002/jrs.4455>
- Correia AM, Clark RJH, Ribeiro MIM, Duarte MLTS (2007) Pigment study by Raman microscopy of 23 paintings by the Portuguese artist Henrique Pousaõ (1859–1884). *J Raman Spectrosc* 38:1390–1405. <https://doi.org/10.1002/jrs.1786>
- Costantini I, Castro K, Madariaga JM (2018) Portable and laboratory analytical instruments for the study of materials, techniques and environmental impacts in mediaeval mural paintings. *Anal Methods* 10:4852–4870. <https://doi.org/10.1039/c8ay00871j>
- Damiani D, Gliozzo E, Turbanti Memmi I (2014) The ‘Madonna and Child Enthroned with Saints’ of Ambrogio Lorenzetti in the St. Augustine Church (Siena, Italy): Raman microspectroscopy and SEM-EDS characterisation of the pigments. *Archaeol Anthropol Sci* 6:363–371. <https://doi.org/10.1007/s12520-014-0175-6>
- Daniel F, Mounier A, Aramendia J, Gómez L, Castro K, Fdez-Ortiz de Vallejuelo S, Schlichte M (2015) Raman and SEM-EDX analyses of the ‘Royal Portal’ of Bordeaux Cathedral for the virtual restitution of the statuary polychromy. *J Raman Spectrosc* 47:162–167. <https://doi.org/10.1002/jrs.4770>
- Daniels V, Stacey R, Middleton A (2004) The blackening of paint containing Egyptian blue. *Stud Conserv* 49:217–230
- David AR, Edwards HGM, Farwell DW, De Faria DLA (2001) Raman spectroscopic analysis of ancient Egyptian pigments. *Archaeometry* 43:461–473. <https://doi.org/10.1111/1475-4754.00029>
- De la Roja JM, San Andrés M, Cubino NS, Santos-Gómez S (2007) Variations in the colorimetric characteristics of verdigris pictorial films depending on the process used to produce the pigment and the type of binding agent used in applying it. *Color Res App* 32:414–423. <https://doi.org/10.1002/col.20345>
- Dei L, Ahle A, Baglioni P, Dini D, Ferroni E (1998) Green degradation products of azurite in wall paintings: identification and conservation treatment. *Stud Conserv* 43:80–88
- DeLaine J (2021) Production, transport and on-site organisation of Roman mortars and plasters. *Archaeol Anthropol Sci*. <https://doi.org/10.1007/s12520-021-01401-5>
- Doménech A, Doménech-Carbó MT, Edwards HGM (2008) Quantitation from Tafel analysis in solid-state voltammetry - application to the study of cobalt and copper pigments in severely damaged frescoes. *Anal Chem* 80:2704–2716. <https://doi.org/10.1021/ac7024333>
- Domingo Sanz I, Chieli A (2021) Characterising the pigments and paints of prehistoric artists. *Archaeol Anthropol Sci*. <https://doi.org/10.1007/s12520-021-01397-y>
- Dominguez-Vidal A, de la Torre-López MJ, Campos-Suñol MJ, Rubio-Domene R, Ayora-Cañada MJ (2013) Decorated plasterwork in the Alhambra investigated by Raman spectroscopy: comparative field and laboratory study. *J Raman Spectrosc* 45:1006–1012. <https://doi.org/10.1002/jrs.4439>
- Ergenç D, Fort R, Varas-Muriel MJ, Alvarez de Buergo M (2021) Mortars and plasters – how to characterise aerial mortars and plasters. *Archaeol Anthropol Sci*. <https://doi.org/10.1007/s12520-021-01398-x>
- Fioretti G, Raneri S, Pinto D, Mignozzi M, Mauro D (2020) The archaeological site of St Maria Veterana (Triggiano Southern Italy) archaeometric study of the wall paintings for the historical reconstruction. *J Archaeol Sci Reports* 29:102080. <https://doi.org/10.1016/j.jasrep.2019.102080>
- FitzHugh EW, Zycherman LA (1983) An early man-made blue pigment from China - barium copper silicate. *Stud Conserv* 28:15–23
- FitzHugh EW, Zycherman LA (1992) A purple barium copper silicate pigment from early China. *Stud Conserv* 37:145–154
- Gasanova S, Pagès-Camagna S, Andriotti M, Hermon S (2018) Non-destructive in situ analysis of polychromy on ancient Cypriot sculptures. *Archaeol Anthropol Sci* 10:83–95. <https://doi.org/10.1007/s12520-016-0340-1>
- Gettens RJ, FitzHugh EW (1993a) Malachite and Green Verditer. In: Roy A (ed) *Artist’s pigments. A handbook of their history and characteristics*. Vol. 2. National Gallery of Art, Washington, Archetype Publications, London, pp 183–202
- Gettens RJ, FitzHugh EW (1993b) Azurite and blue verditer. In: Roy A (ed) *Artist’s pigments. A handbook of their history and characteristics*. Vol. 2. National Gallery of Art, Washington, Archetype Publications, London, pp 23–35
- Gettens RJ, Stout GL (1958) A monument of Byzantine wall painting - the method of construction. *Stud Conserv* 3:107–119
- Gilbert B, Denoël S, Weber G, Allart D (2003) Analysis of green copper pigments in illuminated manuscripts by micro-Raman spectroscopy. *Analyst* 128:1213–1217. <https://doi.org/10.1039/b306138h>
- Gliozzo E (2021) Pigments – Mercury-based red (cinnabar-vermilion) and white (calomel) and their degradation products. *Archaeol Anthropol Sci*. <https://doi.org/10.1007/s12520-021-01402-4>
- Gliozzo E, Burgio L (2021) Pigments – Arsenic-based yellows and reds. *Archaeol Anthropol Sci*. <https://doi.org/10.1007/s12520-021-01431-z>

- Gliozzo E, Ionescu C (2021) Pigments – Lead-based whites, reds, yellows and oranges and their alteration phases. *Archaeol Anthropol Sci*. <https://doi.org/10.1007/s12520-021-01407-z>
- Gliozzo E, Pizzo A, La Russa MF (2021) Mortars, plasters and pigments – Research questions and sampling criteria. *Archaeol Anthropol Sci*. <https://doi.org/10.1007/s12520-021-01393-2>
- Guerra I, Cardell C (2015) Optimizing use of the structural chemical analyser (variable pressure FESEM-EDX Raman spectroscopy) on micro-size complex historical paintings characterization. *J Microsc* 260(1):47–61. <https://doi.org/10.1111/jmi.12265>
- Hatton GD, Shortland AJ, Tite MS (2008) The production technology of Egyptian blue and green frits from second millennium BC Egypt and Mesopotamia. *J Archaeol Sci* 35:1591–1604. <https://doi.org/10.1016/j.jas.2007.11.008>
- Hawthorne FC, Goat LA (1986) The crystal structure and chemical composition of cumengeite. *Mineral Mag* 50:157–162
- Hedegaard SB, Delbey T, Brons C, Rasmussen KL (2019) Painting the Palace of Apries II: ancient pigments of the reliefs from the Palace of Apries. *Lower Egypt Herit Sci* 7:54. <https://doi.org/10.1186/s40494-019-0296-4>
- Herm C (2020) Emerald green versus Scheele's green: evidence and occurrence. Proceedings of the 7th interdisciplinary ALMA conference, Bratislava, Slovakia, October 17–19, 2019 – *Acta Artis Academica* 2020, 189–202.
- Heydenreich G, Spring M, Stillhammerova M, Pina CM (2005) Malachite pigment of spherical particle form. ICOM Committee for Conservation the 14th triennial meeting 12–16 September 2005. *Hague Earthscan* 1:480–488
- Heydenreich G (2013) A note on schifergrün. *Stud Conserv* 48(4):227–236. <https://doi.org/10.1179/sic.2003.48.4.227>
- Holakooei P, Karimy AH (2015) Micro-Raman spectroscopy and X-ray fluorescence spectrometry on the characterization of the Persian pigments used in the pre-seventeenth century wall paintings of Masjid-i Jāme of Abarqū, central Iran. *Spectrochim Acta A* 134:419–427. <https://doi.org/10.1016/j.saa.2014.06.123>
- Holakooei P, de Lapérouse J-F, Rugiadi M, Carò F (2018) Early Islamic pigments at Nishapur, north-eastern Iran: studies on the painted fragments preserved at The Metropolitan Museum of Art. *Archaeol Anthropol Sci* 10:175–195. <https://doi.org/10.1007/s12520-016-0347-7>
- Holakooei P, Karimy AH, Saeidi-Anaraki F, Vaccaro C, Sabatini F, Degano I, Colombini MP (2020) Colourants on the wall paintings of a mediæval fortress at the mount Sofeh in Isfahan, central Iran. *J Archaeol Sci Reports* 29:102065. <https://doi.org/10.1016/j.jas-rep.2019.102065>
- Hradil D, Hradilová J, Bezdička P, Švarcová S (2008) Provenance study of Gothic paintings from North-East Slavakia by handheld X-ray fluorescence, microscopy and X-ray microdiffraction. *X-Ray Spectrom* 37:376–382. <https://doi.org/10.1002/xrs.1014>
- Hradil D, Hradilová J, Švarcová S, Bezdička P, Čermáková Z, Bartlová M (2012) Gothic painted decorations in the gallery of the castle in Lidzbark Wamiński. A Bohemian track in northern Poland II.: materials signs of provenance. Proceedings of the 4th interdisciplinary ALMA conference, November 21–23, 2012, Prague, Czech Republic. *Acta Artis Academica* 2012, 71–78.
- Hradil D, Hradilová J, Kočí E, Švarcová S, Bezdička P, Maříková-Kubková J (2013) Unique pre-Romanesque murals in Kostofány pod Trábečom, Slovakia: the painting technique and causes of damage. *Archaeometry* 55:691–706. <https://doi.org/10.1111/j.1475-4754.2012.00704.x>
- Kiseleva IA, Ogorodova LP, Melchakova LV, Bisengaliva MR, Becturganov NS (1992) Thermodynamic properties of copper carbonates – malachite $\text{Cu}_2(\text{OH})_2\text{CO}_3$ and azurite $\text{Cu}_3(\text{OH})_2(\text{CO}_3)_2$. *Phys Chem Miner* 19:322–333
- Knapp CW, Christidis GE, Venieri D, Gounaki I, Gibney-Vamvakari J, Stillings M, Photos-Jones E (2021) The ecology and bioactivity of some Greco-Roman medicinal minerals: the case of Melos earth pigments. *Archaeol Anthropol Sci*. <https://doi.org/10.1007/s12520-021-01396-z>
- Košařová V, Hradil D, Němec I, Bezdička P, Kanický V (2013) Microanalysis of clay-based pigments in painted artworks by the means of Raman spectroscopy. *J Raman Spectrosc* 44:1570–1577. <https://doi.org/10.1002/jrs.4381>
- Krätchmer A, Odnevall Wallinder I, Leygraf C (2002) The evaluation of outdoor copper patina. *Corros Sci* 44:425–450. [https://doi.org/10.1016/S0010-938X\(01\)00081-6](https://doi.org/10.1016/S0010-938X(01)00081-6)
- Krause W (2006) X-ray powder diffraction data for bottalackite. *Powder Diffr* 21:59–62. <https://doi.org/10.1154/1.2104548>
- Krekel C, Polborn K (2003) Lime blue - a mediæval pigment for wall paintings? *Stud Conserv* 48:171–182
- Kriznar A, Ruiz-Conde A, Sánchez-Soto PJ (2008) Microanalysis of Gothic mural paintings (15th century) in Slovenia: investigation of the technique used by the masters. *X-Ray Spectrom* 37:360–369. <https://doi.org/10.1002/xrs.1050>
- Kühn H (1993) Verdigris and copper resinate. In: Roy A. (ed) *Artists' pigments: a handbook of their history and characteristic*, vol. 2, Oxford University Press
- La Russa MF, Ruffolo SA (2021) Mortars and plasters – how to characterise mortars and plasters degradation. *Archaeol Anthropol Sci*. <https://doi.org/10.1007/s12520-021-01405-1>
- Lancaster LC (2021) Mortars and plasters – how mortars were made. The literary sources. *Archaeol Anthropol Sci*. <https://doi.org/10.1007/s12520-021-01395-0>
- Lauwers D, Garcia Hutado A, Tanevska V, Moens L, Bersani D, Vandenberghe P (2014) Characterisation of a portable Raman spectrometer for in situ analysis of art objects. *Spectrochim Acta A* 118:294–301. <https://doi.org/10.1016/j.saa.2013.08.088>
- Lepot L, Denoël S, Gilbert B (2006) The technique of the mural paintings of the Tournai Cathedral. *J Raman Spectrosc* 37:1098–1103. <https://doi.org/10.1002/jrs.1578>
- Lliveras A, Torrents A, Giráldez P, Vendrell-Saz M (2010a) Evidence for the use of Egyptian blue in an 11th century mural altarpiece by SEM-EDS, FTIR and SR XRD (Church of Sant Pere, Terrassa, Spain). *Archaeometry* 52:308–319. <https://doi.org/10.1111/j.1475-4754.2009.00481.x>
- Lliveras A, Boularand S, Andreotti A, Vendrell-Saz M (2010b) Degradation of azurite in mural paintings: distribution of copper carbonate, chlorides and oxalates by SRFTIR. *Appl Phys A* 99:363–375. <https://doi.org/10.1007/s00339-010-5673-5>
- MacTaggart P, MacTaggart A (1980) Refiners' verditers. *Stud Conserv* 25:37–45
- Marcaida I, Maguregui M, Morillas H, Prieto-Taboada N, de Vallejo SF, Veneranda M et al (2018) In situ non-invasive characterization of the composition of Pompeian pigments preserved in their original bowls. *Microchem J* 139:458–466. <https://doi.org/10.1016/j.microc.2018.03.028>
- Mastrotheodoros GP, Filippaki E, Bassiakos Y, Beltsios KG, Papadopoulou V (2019) Probing the birthplace of the “Epirus school” of painting: analytical investigation of the Filanthropinon monastery murals—part I: pigments. *Archaeol Anthropol Sci* 11:281–2836. <https://doi.org/10.1007/s12520-018-0732-5>
- Mastrotheodoros GP, Beltsios KG, Bassiakos Y (2021) Pigments – iron-based red, yellow and brown ochres. *Archaeological and Anthropological Sciences*. (forthcoming)
- Mattei E, de Vivo G, de Santis A, Gaetani C, Pelosi C, Santamaria U (2008) Raman spectroscopic analysis of azurite blackening. *J Raman Spectrosc* 39:302–306. <https://doi.org/10.1002/jrs.1845>
- Meester de P, Fletcher SR, Skapski AC (1973) Refined crystal structure of tetra-μ-acetato-bis-aquodicyclopentadienylcopper(II). *J Chem Soc, Dalton Trans* 2575–25778. <https://doi.org/10.1039/DT9730002575>
- Moussa AMA, Kantiranis N, Voudouris KS, Stratis JA, Ali MF, Christaras V (2009) The impact of soluble salts on the deterioration of

- pharaonic and coptic wall paintings at Al Qurna, Egypt: mineralogy and chemistry. *Archaeometry* 51:292–308. <https://doi.org/10.1111/j.1475-4754.2008.00422.x>
- Mugnaini S, Bagnoli A, Bensi P, Droghini F, Scala A, Guasparri G (2006) Thirteenth century wall paintings under the Siena Cathedral (Italy). Mineralogical and petrographic study of materials, painting techniques and state of conservation. *J Cult Her* 7:171–185. <https://doi.org/10.1016/j.culher.2006.04.002>
- Murat Z (2021) Wall paintings through the ages. The medieval period (Italy, 12th–15th century). *Archaeol Anthropol Sci*. <https://doi.org/10.1007/s12520-021-01410-4>
- Naumova MM, Pisareva SA, Nechiporenko GO (1990) Green copper pigments of old Russian frescoes. *Stud Conserv* 35:81–88
- Naumova MM, Pisareva SA (1994) A note on the use of blue and green copper compounds in paintings. *Stud Conserv* 39:277–283
- Nevin A, Loring Melia J, Osticioli I, Gautier G, Colombini MP (2008) The identification of copper oxalates in a 16th century Cypriot exterior wall paintings using micro FTIR, micro Raman spectroscopy and gas chromatography-mass spectrometry. *J Cult Herit* 9:154–161. <https://doi.org/10.1016/j.culher.2007.10.002>
- Nicola M, Seymour LM, Aceto M, Priola E, Gobetto R, Masic A (2019) Late production of Egyptian blue: synthesis from brass and its characteristics. *Archaeol Anthropol Sci* 11:5377–5392. <https://doi.org/10.1007/s12520-019-00873-w>
- Nord AG, Tronner K (2018) The frequent occurrence of atacamite in medieval Swedish murals. *Stud Conserv* 63:477–481. <https://doi.org/10.1080/00393630.2018.1444966>
- Nord AG, Tronner K, Billström K, Strandberg Zerpe B (2017) Analysis of mediaeval Swedish paintings influenced by Russian-Byzantine art. *J Cult Her* 23:162–169. <https://doi.org/10.1016/j.culher.2016.07.008>
- Odlyha M, Cohen NS, Foster GM, West RH (2000) Dosimetry of paintings: determination of the degree of chemical change in museum exposed test paintings (azurite tempera) by thermal and spectroscopic analysis. *Termochim Acta* 365:53–63. [https://doi.org/10.1016/S0040-6031\(00\)00613-4](https://doi.org/10.1016/S0040-6031(00)00613-4)
- Ormanci O (2020) Non-destructive characterization of Egyptian blue cakes and wall painting fragments from the east of Lake Van. *Turkey Spectrochim Acta A* 229:117889. <https://doi.org/10.1016/j.saa.2019.117889>
- Orna MV, Low MJD, Baer NS (1980) Synthetic blue pigments: ninth to sixteenth centuries. *I Literature Stud Conserv* 25:53–63
- Pagès-Camagna S, Colinart S (2003) The Egyptian green pigment: its manufacturing process and links to Egyptian blue. *Archaeometry* 45:637–658. <https://doi.org/10.1046/j.1475-4754.2003.00134.x>
- Pagès-Camagna S, Reiche I, Brouder C, Cabaret D, Rossano S, Kanngiesser B, Erko A (2006) New insights into the colour origin of archaeological Egyptian blue and green by XAFS at the Cu K-edge. *X-Ray Spectrom* 35:141–145. <https://doi.org/10.1002/xrs.885>
- Pagès-Camagna S, Laval E, Vigears D, Duran A (2010) Nondestructive and in situ analysis of Egyptian wall paintings by X-ray diffraction and X-ray fluorescence portable systems. *Appl Phys A* 100:671–681. <https://doi.org/10.1007/s00339-010-5667-3>
- Pérez-Alonso M, Castro K, Madariaga JM (2006) Investigation of degradation mechanisms by portable Raman spectroscopy and thermodynamic speciation: the wall painting of Santa María de Lemoniz (Basque Country, North of Spain). *Anal Chim Acta* 571:121–128. <https://doi.org/10.1016/j.aca.2006.04.049>
- Pérez-Arantegui J (2021) Not only wall paintings – pigments for cosmetics. *Archaeol Anthropol Sci*. <https://doi.org/10.1007/s12520-021-01399-w>
- Pérez-Rodríguez JL, Maqueda C, Jiménez de Haro MC, Rodríguez-Rubio P (1998) Effect of pollution on polychromed ceramic statues. *Atmos Environ* 6:993–998. [https://doi.org/10.1016/S1352-2310\(97\)00337-3](https://doi.org/10.1016/S1352-2310(97)00337-3)
- Pérez-Rodríguez JL, del Carmen Jimenez de Haro M, Sigüenza B, Martínez-Blanes JM (2015) Green pigments of Roman mural paintings from Seville Alcazar. *Appl Clay Sci* 116–117:211–219. <https://doi.org/10.1016/j.clay.2015.03.016>
- Pollard AM, Thomas RG, Williams PA (1989) Synthesis and stabilities of the basic copper(II) chlorides atacamite, paratacamite and botallackite. *Mineral Mag* 53:557–563
- Pozza G, Ajo D, Chiari G, De Zuane F, Favaro M (2000) Photoluminescence of the inorganic pigments Egyptian blue, Han blue and Han purple. *J Cul Her* 1:393–398. [https://doi.org/10.1016/S1296-2074\(00\)01095-5](https://doi.org/10.1016/S1296-2074(00)01095-5)
- Pradell T, Salvado N, Hatton GD, Tite MS (2006) Physical processes involved in production of the ancient pigment, Egyptian blue. *J Am Ceram Soc* 89:1426–1431. <https://doi.org/10.1111/j.1551-2916.2005.00904.x>
- Prasartset C (1990) The investigation of pigments and paint layer structures of mural paintings at Maitepnimit Temple. *J National Res Counc Thailand* 22:73–86
- Prati S, Sciutto G, Bonacini I, Mazzeo R (2016) New frontiers in application of FTIR microscopy for characterization of cultural heritage materials. *Top Curr Chem (z)* 374:26. <https://doi.org/10.1007/s41061-016-0025-3>
- Preis W, Gamsjäger H (2002) Solid-solute phase equilibria in aqueous solution. XVI. Thermodynamic properties of malachite and azurite – predominance diagrams for the system Cu²⁺-H₂O-CO₂. *J Chem Thermodyn* 34:631–650. <https://doi.org/10.1006/jcht.2002.0928>
- Riederer J (1997) Egyptian Blue. In: FitzHugh EW (ed) *Artists' pigments*. National Gallery of Art and New York: Oxford University Press, Washington, vol. 3, pp 23–46
- Salvadó N, Pradell T, Pantos E, Papiz MZ, Molera J, Seco M, Vendrell-Saz M (2002) Identification of copper-based green pigments in Jaume Huguet's Gothic altarpieces by Fourier transform infrared microspectroscopy and synchrotron radiation X-ray diffraction. *J Synchrotron Rad* 9:215–222. <https://doi.org/10.1107/S0909049502007859>
- Salvadori M, Sbrilli C (2021) Wall paintings through the ages. The Roman period: republic and early empire. *Archaeol Anthropol Sci*. <https://doi.org/10.1007/s12520-021-01411-3>
- Samanian K (2015) Identification of green pigment used in Persian wall paintings (AD 1501–1736) using PLM, FTIR, SEM/EDX and GC-MS techniques. *Archaeometry* 57:740–758. <https://doi.org/10.1111/arc.12102>
- Scott DA (2002) *Copper and bronze in art – corrosion, colorants, conservation*. Getty Publications, Los Angeles
- Scott DA (2016) A review of ancient Egyptian pigments and cosmetics. *Stud Conserv* 61:185–202. <https://doi.org/10.1179/2047058414Y.0000000162>
- Shortland AJ (2006) Application of lead isotope analysis to a wide range of Late Bronze Age Egyptian materials. *Archaeometry* 48:657–669. <https://doi.org/10.1111/j.1475-4754.2006.00279.x>
- Schiegl S, Weiner KL, El Goresy A (1989) Discovery of copper chloride cancer in ancient Egyptian polychromic wall paintings and faience: a developing archaeological disaster. *Sci Nat* 76:393–400. <https://doi.org/10.1007/BF00366160>
- Smieska L, Mullett R, Ferri L, Woll AR (2017) Trace elements in natural azurite pigments found in illuminated manuscript leaves investigated by synchrotron X-ray fluorescence and diffraction mapping. *Appl Phys A* 123:484. <https://doi.org/10.1007/s00339-017-1093-0>
- Syta O, Wagner B, Bulska E, Zielińska D, Żukowska GZ, Gonzalez J, Russo R (2018) Elemental imaging of heterogeneous inorganic archaeological samples by means of simultaneous laser induced breakdown spectroscopy and laser ablation inductively coupled plasma mass spectrometry measurements. *Talanta* 179:784–791. <https://doi.org/10.1016/j.talanta.2017.12.011>

- Šimůnková E, Bayerová T (2014) Pigmenty (Pigments) STOP, Praha (in Czech)
- Švarcová S, Hradil D, Hradilová J, Kočí E, Bezdička P (2009) Micro-analytical evidence of origin and degradation of copper pigments found in Bohemian Gothic murals. *Anal Bioanal Chem* 395:2037–2050. <https://doi.org/10.1007/s00216-009-3144-7>
- Švarcová S, Kočí E, Bezdička P, Hradil D, Hradilová J (2010) Evaluation of laboratory powder X-ray micro-diffraction for applications in the field of cultural heritage and forensic science. *Anal Bioanal Chem* 398:1061–1076. <https://doi.org/10.1007/s00216-010-3980-5>
- Švarcová S (2011) Preparation, identification and degradation of copper-based inorganic painting pigments. Dissertation. Institute of Chemical Technology, Prague
- Švarcová S, Klementová M, Bezdička P, Łasocha W, Dušek M, Hradil D (2011) Synthesis and characterization of single crystals of the layered copper hydroxide acetate $\text{Cu}_2(\text{OH})_3(\text{CH}_3\text{COO})\cdot\text{H}_2\text{O}$. *Cryst Res Technol* 46:1051–1057. <https://doi.org/10.1002/crat.201100262>
- Švarcová S, Bezdička P, Hradil D (2012) Origin, composition and stability of copper pigments in wall paintings. Proceedings of the 4th interdisciplinary ALMA conference, Prague, Czech Republic, November 21–23, 2012 – Acta Aertis Academica 2012, 213–226.
- Švarcová S, Čermáková Z, Hradilová J, Bezdička P, Hradil D (2014) Non-destructive micro-analytical differentiation of copper pigments in paint layers of works of art using laboratory-based techniques. *Spectrochim Acta A* 132:514–525. <https://doi.org/10.1016/j.saa.2014.05.022>
- Thompson DV (1956) The materials and techniques of mediaeval painting. Dover Publications, New York
- Toegel V (2005) Minerály a lokality sběru (Minerals and collection localities). Rubico, Olomouc (in Czech)
- Tomasini EP, Landa CR, Siracusanoc G, Maiera MS (2013) Atacamite as a natural pigment in a South American colonial polychrome sculpture from the late XVI century. *J Raman Spectrosc* 44:637–642. <https://doi.org/10.1002/jrs.4234>
- Vagnini M, Vivani R, Viscuso E, Favazza M, Brunetti BG, Sgamellotti A, Miliani C (2018) Investigation on the process of lead white blackening by Raman spectroscopy, XRD and other methods: study of Cimabue's paintings in Assisi. *Vib Spectrosc* 98:41–49. <https://doi.org/10.1016/j.vibspec.2018.07.006>
- Van Eikema HM (2004) Changing pictures – discoloration in 15th–17th-century oil painting. Archetype Publications, London
- Van Loon A, Speleers L (2011) The use of blue and green verditer in green colours in the midseventeenth-century paintings of the Oranjezaal, The Hague. In: Spring M (ed) Studying old master paintings: technology and practice: the national gallery technical bulletin 30th anniversary conference postprints. Archetype Publications, London, pp 260–268
- Vandenabeele P, Lambert K, Matthys S, Schudel W, Bergmans A, Moens L (2005) In situ analysis of mediaeval wall paintings: a challenge for mobile Raman spectroscopy. *Anal Bioanal Chem* 383:707–712. <https://doi.org/10.1007/s00216-005-0045-2>
- Velebil D (2008) Chessy ve Francii – světoznámé naleziště azuritu (Chessy in France – the world-famous azurite deposit). *Minerál XVI*:256–261 (in Czech)
- Verri G (2009) The spatially resolved characterisation of Egyptian blue, Han blue and Han purple by photo-induced luminescence digital imaging. *Anal Bioanal Chem* 394:1011–1021. <https://doi.org/10.1007/s00216-009-2693-0>
- Vettori S, Bracci S, Cantisani E, Conti C, Ricci M, Caggia MP (2019) Archaeometric and archaeological study of painted plaster from the Church of St. Philip in Hierapolis of Phrygia (Turkey). *J Archaeol Sci Reports* 24:869–878. <https://doi.org/10.1016/j.jas-rep.2019.03.008>
- Vitti P (2021) Mortars and masonry - Structural lime and gypsum mortars in Antiquity and Middle Ages. *Archaeological and Anthropological Sciences*. <https://doi.org/10.1007/s12520-021-01408-y>
- Wille G, Schmidt U, Hollricher O (2018) RISE: correlative confocal Raman and scanning electron microscopy. In: Toporski J, Dieing T, Hollricher O (eds) Confocal Raman microscopy. Springer series in surface sciences, vol 66. Springer, Cham, pp 559–580. https://doi.org/10.1007/978-3-319-75380-5_23
- Villar SEJ, Edwards HGM (2005) An extensive colour palette in Roman villas in Burgos, Northern Spain: a Raman spectroscopic analysis. *Anal Bioanal Chem* 382:283–289. <https://doi.org/10.1007/s00216-004-2876-7>
- Wagner B, Kępa L, Donten M, Wrzosek B, Żukowska GZ, Lewandowska A (2019) Laser ablation inductively coupled plasma mass spectrometry appointed to subserve pigment identification. *Microchem J* 146:279–285. <https://doi.org/10.1016/j.microc.2018.12.061>
- Wang N, He L, Egel E, Simon S, Rong B (2014) Complementary analytical methods in identifying gilding and painting techniques of ancient clay-based polychromic sculptures. *Microchem J* 114:125–140. <https://doi.org/10.1016/j.microc.2013.12.011>
- Winkler EM (1994) Stone in architecture, properties, durability. 3rd ed, Springer-Verlag, Berlin
- Wong L, Agnew N (eds) (2013) Chapter 13 original materials and techniques. In: The conservation of cave 85 at the Mogao Grottoes, Dunhuang: a collaborative project of the Getty Conservation Institute and the Dunhuang Academy. Getty Publications, Los Angeles, pp 155–190
- Xia Y, Ma Q, Zhang Z, Liu Z, Feng J, Shao A, Wang W, Fu Q (2014) Development of Chinese barium copper silicate pigments during the Qin Empire based on Raman and polarized light microscopy studies. *J Archaeol Sci* 49:500–509. <https://doi.org/10.1016/j.jas.2014.05.035>
- Yong L (2012) Copper trihydroxychlorides as pigments in China. *Stud Conserv* 57:106–111. <https://doi.org/10.1179/2047058411Y.0000000008>
- Zhang Z, Ma Q, Berke H (2019) Man-made blue and purple barium copper silicate pigments and the pabstite ($\text{BaSnSi}_3\text{O}_9$) mystery of ancient Chinese wall paintings from Luoyang. *Herit Sci* 7:97. <https://doi.org/10.1186/s40494-019-0340-4>
- Zoppi A, Lofrumento C, Mendes NFC, Castellucci EM (2010) Metal oxalates in paints: a Raman investigation on the relative reactivities of different pigments to oxalic acid solutions. *Anal Bioanal Chem* 397:841–849. <https://doi.org/10.1007/s00216-010-3583-1>

Publisher's note Springer Nature remains neutral with regard to jurisdictional claims in published maps and institutional affiliations.